

Paleoceanography and Paleoclimatology

RESEARCH ARTICLE

10.1029/2021PA004246

Key Points:

- High-resolution calcareous nannoplankton record reveal upwelling-related primary productivity variations not previously described
- Multiproxy integration allows the assessment of the control by major atmospheric circulation changes at orbital and suborbital timescales
- Reductions in surface productivity during abrupt cold episodes is the result of upwelling limitation by hydrological changes

Correspondence to:

A. González-Lanchas,
lanchas@usal.es

Citation:












González-Lanchas, A., Flores, J.-A., Sierro, F. J., Sánchez Goñi, M. F., Rodrigues, T., Ausín, B., et al. (2021). Control mechanisms of primary productivity revealed by calcareous nannoplankton from marine isotope stages 12 to 9 at the Shackleton Site (IODP Site U1385). *Paleoceanography and Paleoclimatology*, 36, e2021PA004246. <https://doi.org/10.1029/2021PA004246>

Received 20 FEB 2021
 Accepted 23 MAY 2021

© 2021. The Authors.

This is an open access article under the terms of the [Creative Commons Attribution License](#), which permits use, distribution and reproduction in any medium, provided the original work is properly cited.

Control Mechanisms of Primary Productivity Revealed by Calcareous Nannoplankton From Marine Isotope Stages 12 to 9 at the Shackleton Site (IODP Site U1385)

A. González-Lanchas¹ , J.-A. Flores¹ , F. J. Sierro¹ , M. F. Sánchez Goñi^{2,3} , T. Rodrigues^{4,5} , B. Ausín¹ , D. Oliveira^{4,5} , F. Naughton^{4,5} , M. Marino⁶ , P. Maiorano⁶ , and B. Balestra^{7,8,9} 

¹Departamento de Geología, Universidad de Salamanca, Salamanca, Spain, ²École Pratique des Hautes Études (EPHE, PSL University), Pessac, France, ³Université Bordeaux, Environnements et Paléoenvironnements Océaniques et Continentaux (EPOC), UMR 5805, Pessac, France, ⁴Centro de Ciências do Mar (CCMAR), Universidade do Algarve, Faro, Portugal, ⁵Divisão de Geologia e Georecursos Marinhos, Instituto Português do Mar e da Atmosfera (IPMA), Algés, Portugal, ⁶Dipartimento di Scienze della Terra e Geoambientali, Università degli Studi di Bari Aldo Moro, Bari, Italy, ⁷Department of Environmental Science, American University, Washington, DC, USA, ⁸Paleobiology Department, National Museum of Natural History (NMNH) Smithsonian, Washington, DC, USA, ⁹Institute of Marine Sciences Department, University of California Santa Cruz, Santa Cruz, CA, USA

Abstract Nowadays, primary productivity variations at the SW Iberian Margin (IbM) are primarily controlled by wind-driven upwelling. Thus, major changes in atmospheric circulation and wind regimes between the Marine Isotope Stages (MIS) 12 and 9 could have driven substantial changes in phytoplankton productivity which remains poorly understood. We present a high-resolution calcareous nannofossil record from the Shackleton Site Integrated Ocean Discovery Program Site U1385 that allow the assessment of primary productivity and changing surface conditions on orbital and suborbital timescales over the SW IbM. These records are directly compared and integrated with terrestrial – Mediterranean forest pollen – and marine – benthic and planktic oxygen stable isotopes ($\delta^{18}\text{O}$), alkenone concentration [C_{37}], U^{k}_{37} –Sea Surface Temperature and % $\text{C}_{37:4}$ – proxy records from Site U1385. Our results indicate intra-interglacial increase in primary productivity together with intensification of the Azores anticyclonic high-pressure cell beyond the summer that suggests a two-phase upwelling behavior during the full interglacial MIS 11c (~420–397 ka), potentially driven by atmospheric NAO-like variability. Primary productivity is largely enhanced during the inception of glacial MIS 10 and the early MIS 10 (~392–356 ka), linked to intensified upwelling and associated processes during a period of strengthened atmospheric circulation. In agreement with the conditions observed during Heinrich events of the last glacial cycle, primary productivity reductions during abrupt cold episodes, including the Heinrich-type (Ht) events 4 to 1 (~436, 392, 384 and 339 ka) and the Terminations V and IV, seems to be the result of halocline formation induced by meltwater arrival, reducing the regional upward nutrient transference.

1. Introduction

Reconstruction of changes in marine primary productivity during the Pleistocene is crucial for understanding the climate dynamics on glacial/interglacial (G/I) and suborbital timescales (e.g., Beaufort et al., 1997; Kinkel et al., 2000; Molfino & McIntyre, 1990) and the effect of the ocean biological pump on the evolution of atmospheric CO_2 (e.g., Mix, 1989). Given proliferation of coccolithophores, a major group of calcifying phytoplankton, is tightly related to changing surface physicochemical conditions (i.e., light, nutrient concentration, salinity, temperature and turbulence), high resolution records of coccolithophore calcite plates (coccoliths) provide a valuable tool for paleoclimate and paleoceanographic reconstructions (e.g., Baumann & Freitag, 2004; Flores et al., 1997).

The Iberian Margin (IbM) is a benchmark region for the assessment of possible links between Northern Hemisphere and mid-latitude climatic signals (e.g., Martrat et al., 2007; Rodrigues et al., 2011). Crucial atmospheric and hydrological systems in the North Atlantic affect the IbM, as (i) the Iberian Canary Current eastern boundary upwelling (see Relvas et al., 2007) triggering the upwelling of cold and nutrient-rich subsurface waters during spring/summer at the IbM (May to September; Abrantes & Moita, 1999; Moita

et al., 2010; Silva et al., 2009); (ii) the surface ocean boundary between the subpolar and subtropical gyres (Ruddiman & McIntyre, 1981) and (iii) the proximity to the southernmost limit where northern hemisphere icebergs have reached and melted, favoring the accumulation of high quantities of ice-rafted detritus (IRD) and the surface influence of meltwaters in this region (e.g., Lebreiro et al., 1996; Martrat et al., 2007; Shackleton et al., 2000; Vautravers & Shackleton, 2006). Thus, primary productivity variations at the IbM during extended intervals of the Pleistocene could be the result of substantial atmospheric and hydrological changes in the North Atlantic region.

Previous studies for the last glacial cycle and former periods of the Pleistocene at the IbM (e.g., Incarbona et al., 2010; Pailler & Bard, 2002) observed contrasted scenarios of reduced/increased primary productivity during respectively interglacials/transitional stages and glacials. Pailler and Bard (2002) linked this to the enhanced wind-driven upwelling controlled by shifts in the atmospheric circulation patterns over the North Atlantic, that were favored by substantial changes in northern hemisphere ice volume. Further work of Cavaleiro et al. (2020) observed similar patterns of coccolithophore productivity in response to G/I and millennial-scale variability, primarily attributed to variations in the dominant surface water masses and their influence (i.e., changes in nutrient content) on the state of competition between phytoplankton groups, but suggested to be connected to wind-driven upwelling. However, in these studies a clear determination of the mechanisms controlling vertical mixing dynamics and fertilization was severely hampered by the absence of direct information about prevailing wind regimes and atmospheric configuration. Addressing this question requires direct comparison of primary productivity records with those of continental and oceanic conditions derived from the same marine sequence, allowing a better evaluation of the interactions between the atmosphere, ocean and land systems, and modeling validation (e.g., Hernandez et al., 2021). Furthermore, extreme episodes of iceberg calving, such as the Heinrich events of the last glacial cycle or the Heinrich stadial-type events up to the middle Pleistocene, when subpolar fronts experimented marked southward displacements down to 40°N (e.g., Eynaud et al., 2009; Naughton et al., 2009; Rodrigues et al., 2011), are known to lead coastal upwelling weakening or cessation by the southward incursion of iceberg-melting waters (e.g., Ausin et al., 2020; Voelker et al., 2010).

The interval between the Marine Isotope Stages (MIS) 12 to 9 (from 450 to 320 ka) is a key period of contrasted warm and cold stages associated with different baseline conditions (i.e., orbital, ice volume, CO₂). It encompasses the Mid-Brunhes event during the glacial/interglacial Termination V (MBE, MIS 12/11, ~430 ka), one of the most puzzling transition of the last 1 million years leading to interglacials marked by warmer climates and higher atmospheric concentrations of pCO₂ than previous interglacials (Barker et al., 2006; Jansen et al., 1986; Jouzel et al., 2007). As such, the full interglacials MIS 11c and MIS 9e were characterized by extreme warming and early temperature maxima, long-lasting stable climate conditions, greenhouse gas concentrations over the pre-industrial Holocene levels, and higher-than-present sea level (McManus et al., 1999; Petit et al., 1999). Indeed, these interglacials have been frequently considered as potential analogs of the Holocene (e.g., Candy et al., 2014; Loutre & Berger, 2003). The later phases of MIS 11 and the inception of glacial MIS 10 is marked by abrupt millennial-scale variability contemporaneous to the ice-sheet build-up (e.g., McManus et al., 1999; Oppo et al., 1998). In contrast with MIS 10, MIS 12 is the most extreme glacial of the Pleistocene, as many marine, ice and terrestrial proxy records evidence (e.g., Lang & Wolff, 2011). A wide array of high-resolution proxy records from marine sedimentary sequences at the IbM has provided extensive knowledge on the impact of these scenarios in the North Atlantic (e.g., de Abreu et al., 2005; Martrat et al., 2007; Rodrigues et al., 2011, 2017). Among them, those from the Shackleton Site Integrated Ocean Discovery Program (IODP) U1385, located at the SW IbM, outstands by the record of millennial-scale climate variability as a prominent feature (e.g., Hodell et al., 2015; Maiorano et al., 2015; Martin-Garcia et al., 2015; Oliveira et al., 2016; Rodrigues et al., 2017). Interestingly, the hydrological fluctuations conditioned by these shifts (e.g., Rodrigues et al., 2011; Voelker et al., 2010) has been recognized to produce major changes in the phytoplankton communities in the region (e.g., Amore et al., 2012; Maiorano et al., 2015; Marino et al., 2014; Palumbo, Flores, Perugia, Petrillo, et al., 2013b). However, little is known about the impacts of such differentiated climate conditions between MIS 12 and 9 on primary productivity through atmospheric and/or hydrologically forced changes on vertical mixing and nutrient fueling.

Here, we present high-resolution calcareous nannofossil records to reconstruct variations in primary productivity and corresponding changes in surface-water dynamics between MIS 12 and MIS 9 (450–320 ka).

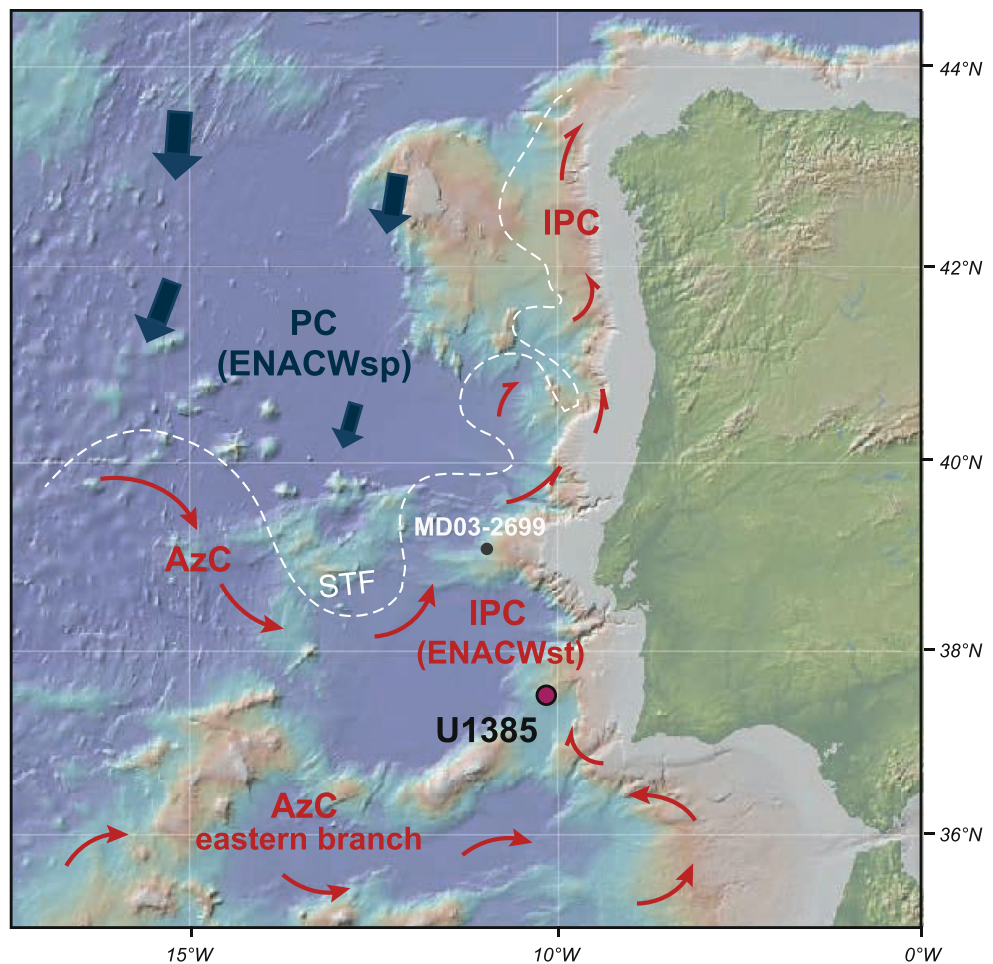


Figure 1. Location of IODP Site U1385 (red dot) and regional winter surface and subsurface circulation scheme off Portugal after Peliz et al. (2005). Modified from Voelker et al. (2010). AzC: Azores Current; ENACW: Eastern North Atlantic Central Water of subtropical (st) or subpolar (sp) component; PC: Portugal Current; IPC: Iberian Poleward Current and STF: Subtropical Front. Site MD03-2699 mentioned in the text is marked with a gray dot. Map source <http://www.geomapapp.org/>.

These data are compared with marine proxies such as alkenone concentration and $U^{k_{37}}$ - Sea Surface Temperature (SST) (Rodrigues et al., 2017) and benthic and planktonic stable oxygen isotope records (Hodell et al., 2015) and terrestrial atmospherically driven vegetation changes from Site U1385 (Desprat et al., 2017; Oliveira et al., 2016; Sánchez-Goñi et al., 2016, 2020). This multi-proxy approach provides an excellent opportunity to evaluate the influence of both atmospheric and hydrological forcing in response to climate oscillations on marine primary productivity in the context of G-I to suborbital/millennial-scale variability.

2. The SW Iberian Margin

The SW IbM is part of the North Atlantic eastern boundary system (Figure 1). The upper 500 m of the water column, including the surface mixed layer and the upper thermocline, is constituted by the Eastern North Atlantic Central Water (ENACW; Fiúza et al., 1998; van Aken, 2001).

Surface to subsurface circulation is modulated by the atmospheric pressure gradients controlled by the relative position and intensity between the Azores High- (AH) and the Iceland Low- (IL) atmospheric pressure cells and the dominant wind patterns (Barton et al., 2001; Fiúza et al., 1998; Relvas et al., 2007). During the winter months, the AH moves southward while IL intensifies, promoting a dominant southerly wind regime over the region (Mason et al., 2005). This configuration results in coastal downwelling conditions

and enhanced northward flux of the Iberian Poleward Current (IPC; Figure 1; Fiúza, 1983). The latter is a recirculating branch of the eastern Azores Current (AzC; Figure 1) that flows northward from September/October to April/March (AzC; Figure 1; Peliz et al., 2005) and includes a subsurface subtropical component of the ENACW (ENACWst) formed by winter cooling at the Azores front (Ríos et al., 1992). As a result, relatively warmer, saltier and oligotrophic surface to subsurface waters bath the region (e.g., van Aken, 2001). During the late spring and summer months (May to September), the northward migration and strengthening of the AH toward the central Atlantic results in prevailing northerly winds. This provokes the intensification of the Portuguese Current (PC; Figure 1), a year-long southward flowing branch of the North Atlantic Current, as well as upwelling of colder and nutrient-rich subsurface waters occurs along the coast (Haynes & Barton, 1990; Peliz et al., 2005; Pérez et al., 2001). The PC involves a subsurface subpolar component of ENACW (ENACWsp) formed by winter cooling in the eastern North Atlantic (McCartney & Talley, 1982). This situation is characterized by the advection of relatively colder, fresher and nutrient-rich waters leading to high primary production (Alvarez et al., 2011; Figueiras et al., 2002; McCartney & Talley, 1982). The resulting upwelling filaments reach up to 200 km offshore (Coste et al., 1986; Fiúza, 1983), a surface distribution covering the location of the Site U1385.

3. Materials and Methods

3.1. Core Material and Chronology

We analyzed sediment samples from Site U1385 (37°34.285' N, 10°7.562'W; 2.578 m below sea level; Figure 1) recovered by the advanced piston corer system of the RV Joides Resolution during IODP Expedition 339 in the SW IbM (Expedition 339 Scientists, 2013). Our study interval corresponds to the depth between 56.34 and 45.9 corrected revised meters composite depth (crmcD).

The lithology of the studied sediments is composed of nannofossil clays and muds, with a variable proportion of biogenic carbonates and terrigenous material (Expedition 339 Scientists, 2013).

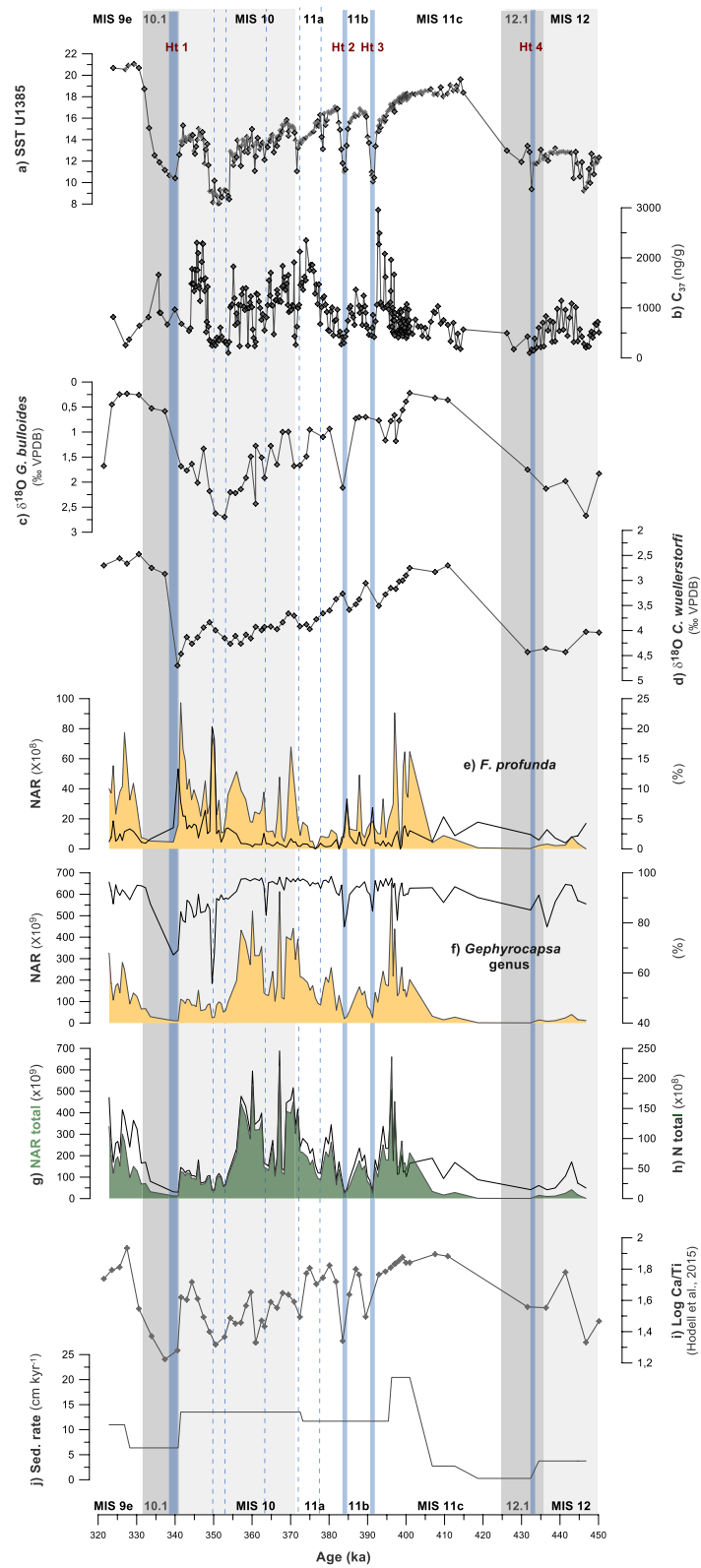
The chronostratigraphic framework followed the age model produced by Hodell et al. (2015), based on the correlation of the benthic oxygen isotope record of Site U1385 with the reference LR04 stack (Lisiecki & Raymo, 2005). The investigated interval spans from 447 ka (late MIS 12) to 323 ka (MIS 9; Lisiecki & Raymo, 2005). G/I stage identification and determination of terminal stadial events 12.1 and 10.1 (corresponding to Terminations V and IV, respectively) in the benthic $\delta^{18}\text{O}$ followed Hodell et al. (2015). The MIS substages corresponds to the nomenclature of Railsback et al. (2015).

Extremely low sedimentation rates are recorded during Termination V and the early MIS 11c (~434–406 ka; Figure 2j), described by Hodell et al. (2015) as a condensed section or hiatus. Thus, interpretations regarding this part of the record – particularly the absolute values of proxies – must be taken with caution.

3.2. Calcareous Nannofossil Analysis

For calcareous nannofossil analyses, a set of 115 samples were subsampled from Holes U1385 A and B evenly spaced every 8 cm. The corresponding temporal resolution of 0.4–0.7 ka (excluding the condensed section) provided the required high-resolution to explore in detail both orbital and millennial-scale climatic variability.

Samples were prepared following the random settling technique outlined by Flores and Sierro (1997). Coccolith identification and quantitative analysis were carried out by using a double polarized-light Nikon Eclipse 80i petrographic microscope at 1000x magnification at the University of Salamanca. A minimum of 400 coccoliths per sample were identified in a variable number of fields of view. A supplementary census count of 10 fields of view was performed to accurately determine the abundance of minor taxa accounting less than 1% of the assemblage. The abundance of specimens from older stratigraphic levels prior to the studied interval, termed reworked nannofossils, were estimated separately. A semiquantitative estimation of coccolith preservation was applied using Scanning Electron Microscope visual observation, following the criteria by Flores and Marino (2002).



Identification of coccolithophore species followed Young et al. (2003) and the guide of coccolithophore biodiversity and taxonomy Nannotax 3 (ina.tmsoc.org/Nannotax3/index.html; Young et al., 2020). Placoliths <3 μm of *Gephyrocapsa* genus were grouped as small *Gephyrocapsa* group following Flores, Bárcena, and Sierro (2000). This cluster mainly contains specimens of *G. aperta* and *G. ericsonii*, and those specimens with a closed central area widely considered as small *G. caribbeanica* (e.g., Saavedra-Pellitero et al., 2017). Occasional small-sized (<3 μm) *G. muelleriae*/*G. margereli* are, as well, included in this cluster; the specimens ≥3 μm of *G. muelleriae*/*G. margereli* are considered themselves in their own group. *Coccolithus pelagicus* subspecies (subsp.) *pelagicus* corresponds to the variety of sizes <10 μm (Geisen et al., 2002; Parente et al., 2004)

Coccolith abundances are presented as percentages (%), coccolith concentration (N; coccolith g⁻¹) and Nannofossil Accumulation Rates (NAR; coccolith cm⁻² kyr⁻¹; Figures 2g and 2h). N and NAR were calculated according to Flores and Sierro (1997). In the absence of dry bulk density, NAR was calculated considering wet bulk density from the shipboard Gamma Ray Attenuation and the sedimentation rate derived from the age model (Figure 2g). Wet bulk density is regularly used to estimate coccolithophore production (see Grelaud et al., 2009; Maiorano et al., 2015; Marino et al., 2014; Stolz & Baumann, 2010).

3.3. Nannoplankton-Based Proxies and Primary Productivity

Total NAR is a proxy for paleoproductivity reconstruction (e.g., Baumann & Freitag, 2004), whose suitability at the IBM relies on several previous studies (e.g., Amore et al., 2012; Ausín et al., 2020; Marino et al., 2014; Palumbo, Flores, Perugia, Emanuele, et al., 2013a). Higher concentration of coccoliths in surface sediments off Portugal is associated to enhanced nannoplankton production in the overlying water column during upwelling events (e.g., Abrantes & Moita, 1999; Moita, 1993).

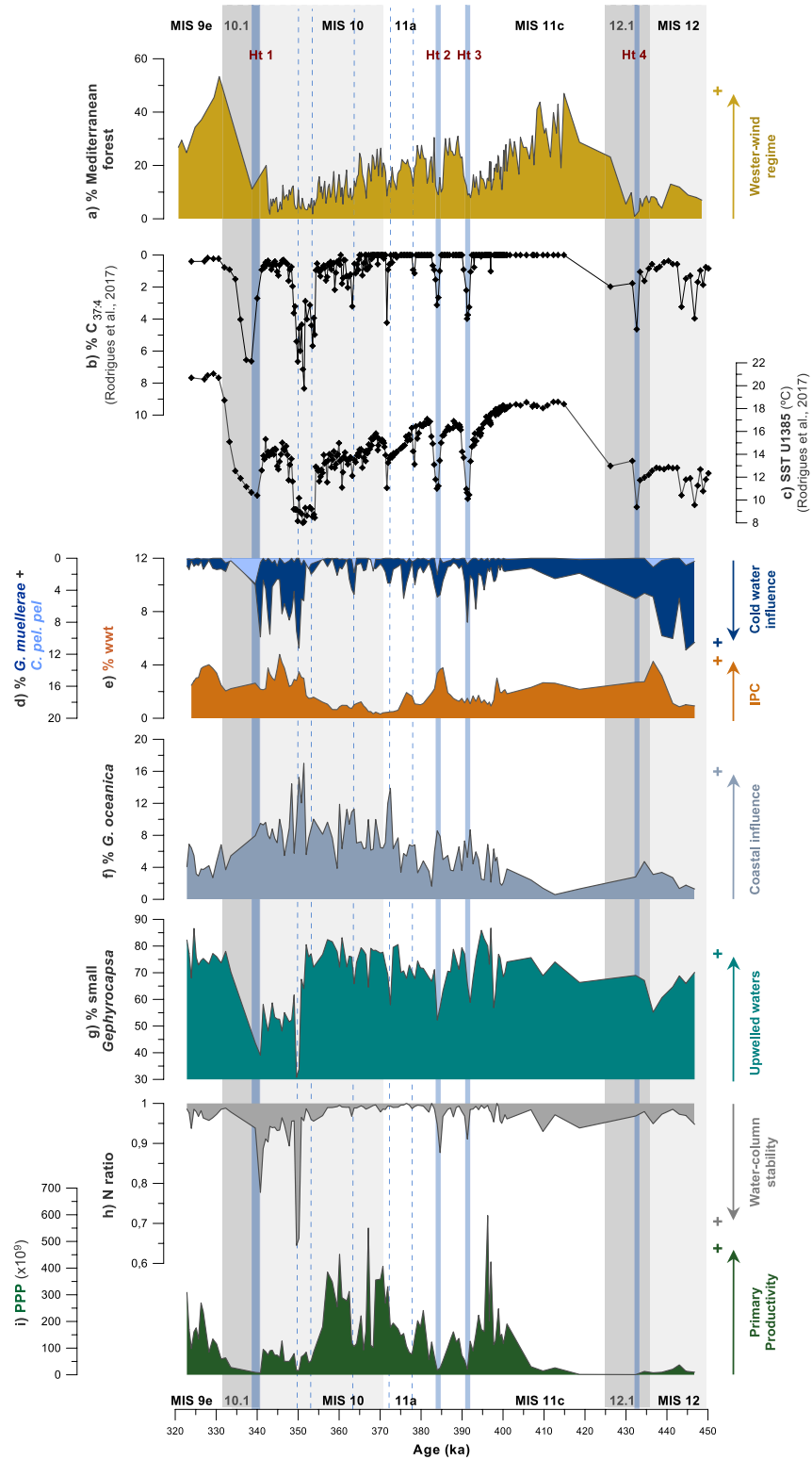
The dominant small *Gephyrocapsa* group (Section 4) is a cluster of r-strategist species with a high affinity for enhanced vertical mixing and/or the availability of highly fertilized upwelled waters in the upper water column (Gartner, 1988; Okada & Wells, 1997). The proportions of this group are here considered an indicator of the availability of highly fertilized surface waters of upwelling origin over the Site U1385. The extant *G. caribbeanica* is believed to have an affinity for ecological conditions comparable to those of the blooming *Emiliania huxleyi* (e.g., Saavedra-Pellitero et al., 2017). In the modern IBM, maximum cell densities of *E. huxleyi* are closely associated with the highest Chl-*a* concentrations (e.g., Guerreiro et al., 2014). Based on these observations, the NAR of small *Gephyrocapsa* and *G. caribbeanica* are grouped together in the primary productivity proxy (PPP; Figure 3i) to increase the accuracy of the upwelling-stimulated coccolithophore primary productivity signal. The species *Gephyrocapsa oceanica* are known to benefit from highly fertilized mature coastal upwelled waters in the modern IBM (Silva et al., 2008).

The species *Florisphaera profunda* is a common inhabitant of the lower photic zone (Kinkel et al., 2000; Okada & Honjo, 1973) widely considered as a tracer of the nutricline depth (e.g., Beaufort et al., 1997; Molino & McIntyre, 1990). We calculated the N ratio, a proxy for nutricline depth fluctuations, following Flores, Bárcena, and Sierro (2000):

$$\text{N ratio} = \text{small placoliths} / \text{small placoliths} + F. \textit{profunda}$$

Small placoliths correspond to specimens of small *Gephyrocapsa*. Higher values of N ratio (Figure 3h) are indicative of a shallower nutricline (Flores, Gersonde, et al., 2000), implying increased availability of nutrients in surface waters.

Figure 2. Calcareous nannoplankton content in the sedimentary record in comparison with sedimentological and geochemical data at Site U1385. (a) Alkenone-based Sea Surface Temperature (SST; Rodrigues et al., 2017). (b) Total alkenone [C₃₇] concentration [ng/g]. (c) Planktic oxygen isotopes (‰ VPDB) from *G. bulloides* (Hodell et al., 2015). (d) Benthic oxygen isotopes (‰ VPDB) from *Cibicidoides wuellerstorfi* (Hodell et al., 2015). Nannofossil Accumulation Rates (NAR; [coccolith g⁻¹ kyr⁻¹]) and relative abundances (%) of (e) *Florisphaera profunda* and (f) *Gephyrocapsa* genus. (g) Nannofossil Accumulation Rates (NAR; [coccolith g⁻¹ kyr⁻¹]) of the total assemblage. (h) Number of coccoliths per gram of sediment (N; [coccolith g⁻¹]) of the total assemblage. (i) Log Ca/Ti (Hodell et al., 2015) and (j) Sedimentation rate (cm kyr⁻¹). Blue bands represent the Heinrich-type (Ht) events 1 to 4 and dashed lines represent other major drops in temperature mentioned in the text.



The species *Oolithotus* spp., *Umbilicosphaera sibogae*, *Umbilicosphaera foliosa* (both grouped here as *Umbilicosphaera* spp.), *Syracosphaera* spp., *Rhabdosphaera clavigera*, *Umbellosphaera* spp. and *Calciosolenia* spp. were lumped together as the warm water taxa (wwt) group (e.g., Amore et al., 2012). This group has a common ecological affinity for tropical to subtropical surface waters (e.g., Baumann et al., 2004; Boeckel & Baumann, 2004; Cachão et al., 2000; Winter, 1994). At the SW IbM, these species are typical in late summer/autumn assemblages (Cachão et al., 2000; Moita et al., 2010; Silva et al., 2008, 2009), tracing the subsurface influence of ENACWst (Fiúza, 1983). Following previous studies (e.g., Amore et al., 2012; Maiorano et al., 2015; Marino et al., 2014; Palumbo, Flores, Perugia, Petrillo, et al., 2013b), the relative abundance of this group in sediments has been already proposed to estimate the influence of the northward flowing IPC and the associated surface to subsurface conditions of lowered nutrient concentration at the studied latitudes. Both, *Gephyrocapsa muelleriae* and *C. pelagicus* subsp. *pelagicus*, are typical markers of cold and less saline surface waters of polar to subpolar origin reaching the IbM latitudes (e.g., Amore et al., 2012; Balestra et al., 2017; Maiorano et al., 2015; Marino et al., 2014; Rodrigues et al., 2010). We consider the relative abundance of these cold temperature-sensitive coccolithophore species to trace the southward displacements of the polar front (PF) and cold-water influence over the studied latitudes.

3.4. Organic Biomarker Analysis

Alkenones are organic biomass compounds synthesized by certain coccolithophore species from the coccolithophore Noëlaerhabdaceae family that remain preserved in sediments (Volkman et al., 1980). The species composing the *Gephyrocapsa* genus are considered to be the main alkenone producers during the studied interval (see Marlowe et al., 1990).

The analytical procedure used for determining alkenone content in sediments is described in detail elsewhere (see Rodrigues et al., 2009; Villanueva et al., 1997). Biomarker analyses were performed in the laboratory of Biogeochemistry at Div.GM-IPMA in 307 sediment levels sampled from Holes U1385 D and E, every 3–4 cm between 56.54 to 46.02 crncd. The total organic compounds were extracted and separated using organic solvents, then identified using Bruker Mass spectrometer detector and quantified with Varian Gas chromatograph Model 3800 equipped with a septum programmable injector and a flame ionization detector with a CPSIL-5 CB column. The concentration of alkenones were determined using *n*-hexatriacontane as an internal standard.

Following different authors (Schubert et al., 1998; Schulte et al., 1999; Villanueva et al., 1998, 2001), the total alkenone concentration [C_{37}] could be representative of the phytoplankton paleoproductivity in open ocean areas.

4. Results

4.1. Nannofossil Assemblages and Proxies

Coccolithophore assemblages at Site U1385 are dominated by *Gephyrocapsa* genus (91.3% on average; Figure 2f). The PPP records 155×10^9 coccoliths $\text{cm}^{-2} \text{kyr}^{-1}$ on average, in the range of previous studies in the region that include this interval of high clacareous nannoplankton production (e.g., Marino et al., 2014). Maxima values are recorded during the late MIS 11, centered at 397 ka, and MIS 10, between 374 and 355 ka, whereas low-to-intermediate values are registered (i) until 400 ka during the early MIS 11c and (ii) MIS 9e, from 332 ka toward the end of the studied interval. Lowest PPP are recorded: (i) throughout the late MIS 12 and TV, between 445 and 425 ka, (ii) in two short episodes centered at 391 and 384 ka during the late MIS 11, and (iii) late MIS 10 and TIV, between 355 and 332 ka (Figure 3i).

Figure 3. Atmospheric and oceanographic proxies at the Site U1385. (a) Relative abundances (%) of mediterranean forest pollen (Desprat et al., 2017; Oliveira et al., 2016; Sánchez Goñi, 2016, 2020). (b) Relative abundances (%) of tetra-unsaturated alkenone ($C_{37:4}$; Rodrigues et al., 2017). (c) Alkenone-based Sea Surface Temperature (SST; Rodrigues et al., 2017). Relative abundance (%) of (d) *G. muelleriae* + *C. pelagicus* subsp. *pelagicus*; (e) warm water taxa (wwt; smoothed curve); (f) *G. oceanica* and (g) small *Gephyrocapsa*. (h) N ratio. (i) Primary productivity proxy (PPP; NAR small *Gephyrocapsa* $\times 10^9$ + NAR *Gephyrocapsa caribbeanica* $\times 10^9$ [coccolith $\text{cm}^2 \text{kyr}^{-1}$]). Substages are indicated according to Railsback et al. (2015). Blue bands represent the Heinrich-type (Ht) events 1 to 4 and dashed lines represent other major drops in temperature mentioned in the text.

The contribution of *F. profunda* accounts for 2.3% of the total assemblage on average, reaching values over 5% at 409, 391 and 384 ka during MIS 11, and at 350 and 341 ka during MIS 10 and MIS 10/MIS 9 transition (Figure 2e). The N ratio oscillates slightly around 0.9 throughout most of the record (Figure 3h). In general, the highest N ratio ~ 0.95 accompanies periods of PPP maxima, while lowered values under 0.9 are identified as short-term episodes together with PPP reductions (Figures 3h and 3i). The lowest N ratio ~ 0.6 , which correspond to the highest percentages of *F. profunda*, are recorded during the MIS 10/MIS 9 transition (TIV) and are accompanied by increases in the NAR of *F. profunda* (Figures 2e and 3h).

Relative abundance of small *Gephyrocapsa* averages 69.2% (with maxima and minima of 86.62% and 30.73%, respectively) through the studied interval, with substantial reductions only recorded during short episodes around 425 ka of the late MIS 12; 397, 391 and 384 ka at MIS 11; 371 ka at MIS 11/MIS 10 and within a more continuous and much lower reduction toward values below 50% between 350 to 338 ka, across MIS 10 (Figure 3g). The percentages of *G. oceanica* averages 6.2% and evidence a strong control for G/I variability (Figure 3f). There is a marked progressive increasing trend from minima values below 5% at the full interglacial MIS 11c to maxima values $\sim 18\%$ at 350 ka during MIS 10 (Figure 3f). Short-term increases are in phase with rapid reductions in % of small *Gephyrocapsa* (Figures 3f and 3g).

The wwt is recorded in low proportion (0.86% on average). The profile is characterized by higher abundances during the late glacial to interglacial periods MIS 12 to MIS 11 (~ 443 – 400 ka) and MIS 10 to MIS 9 (~ 352 – 320 ka). Lowest values are observed between ~ 375 and 352 ka during the MIS 11/10 transition (Figure 3e). Percentages of *G. muellerae* + *C. pelagicus* subsp. *pelagicus*, with contribution to assemblages of, respectively 2.9% and 0.3%, evidence a pattern of short-term moderate increases, with summed values slightly over 10% between ~ 446 and 431 ka during MIS 12, from ~ 391 to 384 ka during late MIS 11, ~ 364 ka during MIS 10 and a more continuous increase between ~ 352 and 339 ka over late MIS 10 and TIV (Figure 3d).

4.2. Alkenone-Based Paleoproductivity

Total alkenone concentration [C_{37}] changes between 101.95 and 2955.57 ng/g through the record, evidencing a pattern of high frequency variability (Figure 2b). The maximum values are detected at the intervals between 396 and 393 ka during the late MIS 11c, 374–355 ka during the MIS 11/10 transition and 347–345 ka at MIS 10. The lowest alkenone concentrations are recorded between 432 and 427 ka during the terminal stadial 12.1, at 414 ka at MIS 11c, at 391, 384 ka during late MIS 11 and between 371 and 353 ka during MIS 10 (Figure 2b).

5. Discussion

The overall G-I variability observed in the PPP record is superimposed by millennial-scale changes (Figure 3i), concomitant to oscillations in other nanoplankton-based proxy records, SST (Rodrigues et al., 2017) and Mediterranean forest percentage profiles from Site U1385 (Desprat et al., 2017; Oliveira et al., 2016; Sánchez Goñi et al., 2016, 2020; Figures 3a and 3c). In general, high PPP values coincide with reduced Mediterranean forest development, (i.e., cold and weak winter precipitation, and low SST during glacials) whereas interglacials are marked by lower PPP values and significant expansion of the Mediterranean forest (i.e., warm and wet winters, and warm SST; Rodrigues et al., 2017; Figures 3a, 3c and 3i).

A prominent feature in our record is the occurrence of abrupt cold events, primarily recognized as abrupt drops in SST (Rodrigues et al., 2017) having a large impact on PPP, which shows substantial reductions (Figures 3c and 3i). The occurrence of Heinrich-type (Ht) events 1 to 4 (~ 436 , 392, 384 and 339 ka) is recognized by the record of abrupt drops in SST together with increased % $C_{37:4}$ (Rodrigues et al., 2017) in comparison with the reference record by Rodrigues et al. (2011) at MD03-2699 (blue bands in Figures 2 and 3). Other short-term SST drops previously described by (Rodrigues et al., 2011; ~ 372 , 350 and 355 ka), or observed in the temperature record for this interval (Rodrigues et al., 2017; ~ 378 and 364 ka) are here identified to have a similar correspondence with lowered PPP (dashed lines in Figures 2 and 3). All these short-term episodes are also detected in the terrestrial realm by strong contraction of the Mediterranean forest, (i.e., winter precipitation decrease, colder atmospheric temperatures; Figure 3a).

The detailed assessment of the control mechanisms on primary productivity in the area of study requires multiple non-excluding influencing factors to be considered: (i) changes in the dominant wind systems and wind-stress stimulating vertical mixing (e.g., Incarbona et al., 2010; Paillet & Bard, 2002); (ii) the nutrient content of the subsurface waters fueling the upwelling (e.g., Palumbo, Flores, Perugia, Petrillo, et al., 2013b); (iii) shifts in the regional hydrological configuration and associated surface-nutrient transport (e.g., Amore et al., 2012; Maiorano et al., 2015; Palumbo, Flores, Perugia, Emanuele, et al., 2013a); (iv) changes in the extension and/or offshore displacement of the coastal upwelling influence area (e.g., Salgueiro et al., 2014); (v) arrival of iceberg-melting waters leading to vertical mixing weakening or even cessation, as observed during extreme deglacial episodes (e.g., Voelker et al., 2009).

In the following sections we provide a detailed discussion about these records and the main processes at hand during G/I cycles, and millennial-scale timescales.

5.1. Atmospheric Patterns Driving Primary Productivity During Interglacials

The parallelism observed between primary productivity, hydrological and atmospheric records (Figure 3) suggests that, as demonstrated for the modern setting (e.g., Guerreiro et al., 2014; Lopes et al., 2009; Oliveira et al., 2009), the intensity and position of the Azores High (AH) pressure cell played a significant role on the vertical mixing and surface nutrient availability at the IbM over different timescales.

Present-day and past changes in the Mediterranean forest composition and development are mainly controlled by winter precipitation and seasonal climate contrast, reflecting changes in the position of the westerlies led by the AH during the winter (Gouveia et al., 2008; Naughton et al., 2009; Oliveira et al., 2018). According to Oliveira et al. (2016), the expansion of the Mediterranean forest, as observed during the early full interglacials MIS 11c and 9e (values over 20%; Figure 3a), is indicative of higher winter precipitation, which, in turn, indicates increased influence of the westerly wind systems and related southward winter position of the AH (Figure 4a). Conversely, forest reductions without a counterpart cooling in the SST, as recorded during the late phase of MIS 11c (Rodrigues et al., 2017; Figures 3a and 3c), are associated with an intensified and northward positioned AH during the winter, with consequent reduction of large-scale winter precipitation in SW Iberia (Oliveira et al., 2016; Figure 4b).

Today, the North Atlantic and Iberian climate are closely coupled through the North Atlantic Oscillation (NAO), the variable pressure gradient between the AH and Icelandic Low (IL) centers during the winter season (Hurrell, 1995; Hurrell et al., 2003). A negative (−) NAO mode implies a weakened North Atlantic atmospheric circulation and the southward displacement of the westerly wind systems down to southern Europe and North Africa during winter (Figure 4a). During a positive (+) NAO mode, the North Atlantic atmospheric circulation is strengthened during the winter and the westerly wind systems are displaced further north (Figure 4b; Hurrell, 1995; Trigo et al., 2002). Consequently, the regional seasonal atmospheric circulation is modulated at decadal to centennial timescales and causes a regional hydrological impact, implying an intensified winter northward IPC, as the result of the southward position and weakening of AH (Barton et al., 2001; Haynes & Barton, 1990; Figure 4a). The prevalence of northerly trade wind regime aside the summer season during + NAO (Figure 4b) has been shown to increase the frequency of the upwelling events in the region (e.g., Alvarez et al., 2009; Barton, 2001; Silva et al., 2008; Vitorino et al., 2002).

5.1.1. Early Interglacials

The early interglacial substages at MIS 11c (~420–400 ka) and MIS 9e (~337–320 ka) are characterized by low to intermediate PPP and a relatively deep nutricline with moderate surface nutrient availability (Figures 3g–3i), also supported by a reduction in the C_{37} alkenone concentration (Figure 2b). These conditions suggest a substantial weakening in the upwelling regime by a weaker northerly trade influence over SW Iberia due to the winter southern position of AH and enhanced westerly influence (Figures 3a and 4a). Such conditions probably led to moderate surface-water stratification, resulting in a prolonged warming of surface waters (Figure 3c). Surface to subsurface oligotrophy and decline in regional vertical mixing were also promoted by the long-term intensified influence of the winter IPC and ENACWst (Figure 3e) and, potentially, by a shallower position of this subsurface water mass system in absence of a strong northerly trade influence during winter (Barton, 2001; Figure 4a). The hampering effect of this hydrological configuration seems to reduce, as well, the arrival of nutrient-rich waters from the PC and/or surface offshore transport

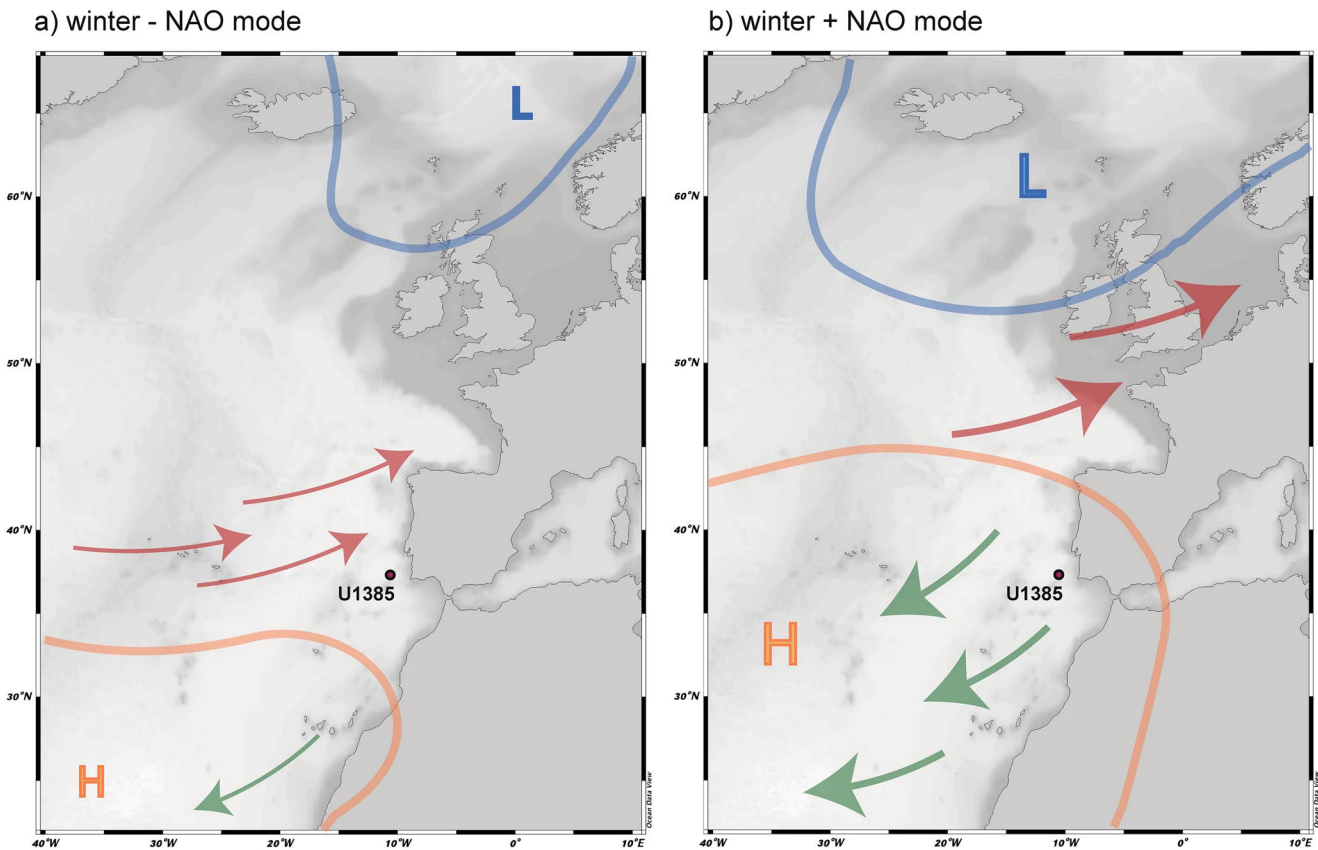


Figure 4. Simplified scheme of the modern patterns of the intensity and position of the Azores anticyclone high-pressure cell (AH) and associated wind regimes at the Iberian Margin (IbM) during the winter entailed by the modern North Atlantic Oscillation (NAO) variability, as in Wanner et al. (2001). Arrow thickness indicates intensity of wind systems. Red: westerly wind system; green: northerly trades. (a) Winter weakening and southward movement of the AH during a negative (–) NAO mode. (b) Winter intensification and northward movement of the AH during a positive (+) NAO mode.

from the neighbor coastal upwelling, a fact that is also sustained by the reduced % *G. oceanica* together with the increased % wwt (Figures 3f and 3e); this later group has been considered to trace intensified ENACWst water mass transport towards Iberia during the winter (e.g., Cachão et al., 2000). Ultimately, both interglacial sea-level high stands during the early MIS 11c and MIS 9e (Rohling et al., 2009) exclude any offshore displacement of the coastal upwelling cells through the position of the Site U1385. A recently suggested increased influence of nutrient-poorer subtropical waters during the full interglacial MIS 11 and 9 to the north of our Site (Cavaleiro et al., 2020) is consistent with our observations. As well, similar primary productivity scenario and associated upwelling conditions was described at the IbM during other more recent interglacial periods (i.e., MIS 5; Pailler & Bard, 2002) and the Holocene (Incarbona et al., 2010).

By analogy with the present-day conditions, the enhanced winter westerlies influence over the IbM, reconstructed during the early stages of interglacials MIS 11c and 9e (Figures 3a and 4a), suggest a control of a prevalent winter – NAO-like (Figure 4a), reducing primary productivity at Site U1385 by the balanced restriction of the upwelling season and associated fertilization processes to the summer months, when the AH intensification occurred.

5.1.2. Intra-Interglacial Shift to the Late MIS 11c

The late phase of the full interglacial MIS 11c (~405–392 ka) is characterized by a shift to high PPP corresponding to a shallow nutricline and consequent increased surface nutrient availability in comparison to the early phase of this substage (Figures 3g–3i). This is also supported by progressively increased C_{37} alkenone concentration (Figure 2b). Increased percentages of cold temperature-sensitive coccolithophore taxa (Figure 3d) are consistent with slightly cooler surface waters. By contrast, the SST record shows a moderate ocean cooling toward the end of the full interglacial (Rodrigues et al., 2017; Figures 3c and 3d).

A reduced influence of the oligotrophic IPC during the winter (Figure 3e) might have provoked a regional eutrophication. The high % of small *Gephyrocapsa* (Figure 3g) characterizes, beyond the general availability of upwelled surface waters, a link for these conditions with an enhanced influence of the nutrient-richer PC (e.g., Amore et al., 2012; Palumbo, Flores, Perugia, Petrillo, et al., 2013b).

A more intense and northernmost positioned AH during winter reduced the westerly influence (Figure 3a) and enhanced the winter northerly trades, that may progressively extend its effect over SW Iberia (Figure 4b). As proposed by Oliveira et al. (2016), this intra-interglacial shift (Figure 3a) without a counterpart cooling in the SST (Rodrigues et al., 2017; Figure 3c) could be explained by a progression toward the prevalence of a + NAO mode (Figure 4b). In agreement with present day observations in the region (e.g., Alvarez et al., 2009; Barton, 2001; Silva et al., 2008; Vitorino et al., 2002), an increased frequency of the upwelling events beyond the summer season is observed coupled to the positive modes of the modern NAO. The increased effect of northerly trades by maintained AH northward position is here interpreted with the prevalence of a + NAO-like mode (Figures 3a and 4b), considered responsible of the enhanced upwelling and increased PPP in a comparable way to the modern conditions. Additionally, widening of the coastal upwelling zones could have occurred as a result of strengthened atmospheric circulation (e.g., Pailler & Bard, 2002), complementary favoring the conditions for primary productivity at Site U1385.

The effect of this intra-interglacial atmospherically shift at the full interglacial MIS 11c over primary productivity records has been similarly identified in the Alboran Sea (González-Lanchas et al., 2020) at around 406 ka via enhanced western Mediterranean circulation and complete upwelling development controlled by this atmospheric shift towards a prevalent + NAO-like configuration.

5.2. Enhanced Primary Productivity at the Onset of Glacial MIS 10

The interval spanning from ~392 to 356 ka from the late MIS 11 to early full glacial MIS 10 (inception to glacial MIS 10) is characterized by a long-term increase in PPP and a shallow nutricline with enhanced surface nutrient availability (Figures 3g–3i), also supported by relatively high values in C_{37} alkenone concentration (Figure 2b). A progressively reduced influence of the AzC waters through the IbM by reduced IPC effect over the studied area during the beginning of MIS 10 is observed from the lowered % wwt (Figure 3e) along with a gradual SST cooling (Rodrigues et al., 2017; Figure 3c).

Growing of ice sheets toward the glacial period, as recorded by the long-term trend toward heavier values of benthic $\delta^{18}O$ (Figure 2d) in agreement with other isotopic records (e.g., Elderfield, et al., 2012; Lisiecki & Raymo, 2005) and the sea-level stack of Spratt and Lisiecki (2016), probably led to an increased meridional air pressure gradient between the high and low latitudes in the North Atlantic (Keffer et al., 1988; Ruddiman, 1977). This atmospheric trend and the climate shift toward cooler and drier conditions in SW Iberia affected the regional vegetation, as evidenced by the reduction of the Mediterranean forest (Figure 3a). Nonetheless, this vegetation pattern toward the glacial (Figure 3a) cannot be solely interpreted as the result of a reduction in the winter humidity (Figure 4), as evidenced by the parallel reduction in SST throughout the glacial onset (Rodrigues et al., 2017; Figure 3c). However, the higher wind stress during transitional and glacial phases is considered a crucial factor determining intensified wind-driven upwelling at the North Atlantic eastern boundary system (e.g., Abrantes, 2000; Bradtmiller et al., 2016; Pailler & Bard, 2002; Romero et al., 2008; Sarnthein et al., 1988). This process could explain the increased PPP and high nutrient content in surface waters through this interval (Figures 3g–3i). Models for the LGM suggest intensification in the AH and the IL (e.g., Hewitt et al., 2001); in this sense, strengthening of the northerly trades over the IbM could explain the enhanced upwelling in a comparable way that the record by Pailler and Bard (2002) at the onset of glacials MIS 4 and 2 at MD9-2042.

Strengthened wind-stress together with reduced winter IPC (Figure 3e), promoting the maintained influence of the surface PC, is considered, as well, to result in the prevalent upward advection of deeper and nutrient-richer subsurface ENACWsp fueling the regional upwelling. This observation is in agreement with nutrient-richer surface waters favoring coccolithophore proliferation against diatoms discussed by Cavaleiro et al. (2020) at the nearby site MD03-2699. Additionally, the strengthened atmospheric circulation could have resulted in substantial widening of the coastal upwelling (e.g., Pailler & Bard, 2002), benefiting eutrophication at Site U1385 due to greater proximity of the upwelled filaments (or area of influence of the upwelling). Ultimately, we cannot discard the possible impact of an offshore displacement of the coastal upwelling cells

during the long-term sea-level drop through glacial MIS 10 (Rohling et al., 2009). The increased percentages of *G. oceanica* toward MIS 10 from the MIS 11 transition (Figure 3f) could be a potential indicator of an increase in the coastal influence, entailing coastal upwelling processes, over the studied location. A similar process was already proposed by Salgueiro et al. (2014) for the LGM. The considerable increase in coccolith accumulation and primary productivity through this interval in comparison with more inshore locations at the early MIS 10 (e.g., Amore et al., 2012; Palumbo, Flores, Perugia, Petrillo, et al., 2013b) supports this process.

Summarizing, a scenario comparable to that observed during the LGM (Ausín et al., 2020; Incarbona et al., 2010; Salgueiro et al., 2014) is proposed for the inception of glacial MIS 10 and the early full glacial MIS 10, in which the enhanced PPP is considered to be the result of several potentially active mechanisms intensifying fertilization due to either increased wind-induced upwelling, increased nutrient content in the source of upwelling and/or enhanced surface nutrient arrival to the Site U1385.

5.3. Impact of Surface Water Conditions on Primary Productivity During Abrupt Cold Events

The availability of upwelled waters reaching Site U1385 is constant through almost the entire interval (Figure 3g), driving eutrophication of the uppermost water column where the dominant *Gephyrocapsa* species inhabits. However, significant reductions in surface water fertilization occurred during the Ht events 4 to 1 (~436, 392, 384 and 339 ka) and other short-term cold episodes, reflected as abrupt decreases in PPP, also supported by reduced C_{37} alkenone concentration, and limited nutrient availability, as recorded by the lowered values in the N ratio and decrease in % *small Gephyrocapsa* (Figures 2d and Figures 3a–3i). The higher percentages of cold-water coccolithophore species (Figure 3d) together with severe SST coolings and increased % of $C_{37:4}$ (Rodrigues et al., 2017; Figures 3c and 3b) suggest pronounced southward shifts of the PF. The influence of ice rafting and the presence of meltwaters at the studied latitudes during extreme cooling events at the studied interval has been already detailed and discussed (de Abreu et al., 2005; Rodrigues et al., 2011, 2017; Voelker et al., 2010). The observed decrease in Ca/Ti (Figure 2h) is indicative of the reduction in carbonate burial, as a result of the reduced surface production (Figures 2b and 3i), but also of the enhancement in detrital input (Hodell et al., 2013, 2015).

Extreme continental aridity and cold atmospheric conditions on land during Ht 4, 3 and 2 (Oliveira et al., 2016; Sánchez Goñi et al., 2016) are here similarly recognized by the abrupt reduction of the Mediterranean forest (Figure 3a) together with low SST (Rodrigues et al., 2017; Figure 3c) during Ht 1, and probably during the other short-term abrupt coolings during the glacial inception of MIS 10 (Figures 2 and 3; dashed lines). The prevailing northerly trade regime over SW Iberia from the extended aridity indicated by the pollen record (Figure 3a) is expected to intensify the coastal upwelling, however, this notion contrast with the lowest PPP and the reduced surface nutrient availability recorded during these episodes (Figures 3f–3i).

The rapid evolution toward surface subpolar cold-water conditions is known to result in unfavorable conditions for calcareous nanoplankton growth in the region (i.e., cold, turbid, and low salinity; see Maiorano et al., 2015; Marino et al., 2014 and references therein). In particular, the higher abundances of *F. profunda* (Figure 2e) in the North Atlantic during the occurrence of Heinrich events are consistent with enhanced upper water-column stability (e.g., Colmenero-Hidalgo et al., 2004; Marino et al., 2014). Synchronous short-term increases in the relative abundances of *G. oceanica* (Figure 3f) could be tentatively interpreted as the effect of a reduction in surface-water salinity (Ausín et al., 2015; Jordan & Winter, 2000) in response to the freshwater advection. However, as suggested by previous authors, a better adaptation of this *Gephyrocapsa* species by means of vertical migration and affinity of this species to deeper water layers in the proximity of the thermocline (e.g., Girardeau et al., 1993), or the variable tolerance of hypothetical sub-species included in this group (e.g., Andrulleit et al., 2003) could not be discarded. The formation of a halocline led by surface freshening, as occurred during the Heinrich events of the last glacial cycle (see Voelker et al., 2009), could explain the recorded conditions where, despite a plausible favorable wind stimulation (Figure 3a), the water column vertical structure with a shallower mixed layer separated from deep nutrient-rich levels would reduce the upward nutrient transference. As in Voelker et al., (2009), the presence of higher-temperature ENACWst underneath the halocline could particularly explain the favorable thermal conditions for the proliferation of *F. profunda* (Figure 2d) and the eventual increases in % wwt observed during the occurrence of these episodes (Figure 3e).

The most extreme and long-lasting of these conditions occurred between 350 ka, at the end of MIS 10, and TIV at the onset of MIS 9 (Figure 3). As previously pointed out (Maiorano et al., 2015), there is a good correspondence of these conditions at ~ 349 ka with IRD deposition at MD01-2446 (Voelker et al., 2010) and Site U1313 (Naafs et al., 2011, 2013; Stein et al., 2009), suggesting analogous conditions with a Heinrich stadial. During the late glacial MIS 12 and TV, despite important SST cooling is solely recorded at ~ 445 and Ht4 (Rodrigues et al., 2017; Figures 3b and 3c), the PPP, N ratio and cold-water coccolithophore species (Figures 3d and 3h) evidence an important reduction in surface production and implementation of surface subpolar conditions between 445 and 425 ka (Figure 3). Among both Terminations, conditions of primary productivity after cold deglacial episodes seems to be more rapidly increased after TIV toward MIS 9 (Figure 3), while TV show a more persistent limited surface-nutrient fertilization into the MIS 11 (Figure 3).

Overall, productivity reduction and associated hydrological and paleoceanographic conditions observed during these abrupt cold events of different duration for the studied interval impacted nanoplankton assemblages on a regional level, as proven by the consistency of our record with that from core MD03-2699 (Cavaleiro et al., 2020). The mechanism that reduces primary productivity is probably comparable to that proposed during the Heinrich episodes of the last glacial (e.g., Ausin et al., 2020; Incarbona et al., 2010).

6. Conclusions

Changes in primary productivity related to variation in wind-induced upwelling at the Site U1385 at the SW IbM during the MIS 12 to 9 interval are reconstructed from the study of calcareous nanoplankton assemblages. The integration with previously published SST and pollen-based vegetation and climate records at the same site evidence that the environmental conditions controlling phytoplankton production were largely influenced by the prevailing atmospheric configuration. During the early stages of the full interglacial MIS 11c (~ 420 – 405 ka) and MIS 9e (~ 337 – 320 ka), moderate primary productivity and surface nutrient availability is the result of reduced vertical mixing and offshore nutrient transport by a restriction of the upwelling stimulation to the summer months own by an atmospheric configuration comparable to a prevailing – NAO-like mode. The full interglacial MIS 11c registers a shift to increased primary productivity and surface nutrient availability (~ 405 – 392 ka), which is attributed to an intra-interglacial AH intensification beyond the summer comparable to a progression to prevailing + NAO modetowards the end of MIS 11. Enhanced primary productivity and surface nutrient availability through the inception and early MIS 10 (~ 392 – 356 ka) indicate upwelling offshore displacement and intensification in the context of strengthened atmospheric circulation during the glacial transition. Significant abrupt reductions in primary productivity and enhanced surface stability are identified during the occurrence of Heinrich-type (Ht) events 4 to 1 (~ 436 , 392, 384 and 339 ka), other short-term cold episodes (~ 378 , 372, 364, 350 and 355 ka) and more prolonged during the Terminations V and IV. The establishment of cold surface subpolar conditions and increased $\% C_{37:4}$ indicates that, as during the Heinrich stadials of the last glacial cycle, the regional halocline formation induced by meltwater arrival restricted the nutrient upward advection.

Acknowledgments

This study was supported by the predoctoral FPU contract FPU17/03349 awarded to A. González-Lanchas by the Spanish Ministry of Science, Innovation and Universities. Essential financial infrastructure was provided by the programs RTI2018-099489-B-100 of the Spanish Ministry of Science, Innovation and Universities granted to GGO (Grupo de Geociencias Oceánicas de la Universidad de Salamanca). T. Rodrigues received funds from Portuguese National Foundation for Science and Technology FCT - through projects: Warm World (PTDC/CTA-GEO/29897/2017) and CCMAR UIDB/04326/2020. D. Oliveira acknowledges funding from Portuguese Foundation for Science and Technology (FCT) through the CCMAR Research Unit - project UIDB/04326/2020 and contract (CEECIND/02208/2017). The authors are grateful to IODP for inviting some of the coauthors to participate in Expedition 339 and providing the samples used in this study. The authors also thank two anonymous reviewers and Carlos Jaramillo, whose constructive comments and suggestions improved the quality of this study.

Data Availability Statement

All original data produced for this work is available at <https://data.mendeley.com/datasets/kv85rjj4y7/3> archived at the public repository Mendeley as: González-Lanchas, Alba; Flores, José-Abel; Sierro, Francisco J. (2021), "High-resolution calcareous nannofossil record between the Marine Isotope Stage (MIS) 12 to 9 from the IODP Site U1385", Mendeley Data, V3, doi: [10.17632/kv85rjj4y7.3](https://doi.org/10.17632/kv85rjj4y7.3)".

References

- Abrantes, F. (2000). 200 000 yr diatom records from Atlantic upwelling sites reveal maximum productivity during LGM and a shift in phytoplankton community structure at 185 000 yr. *Earth and Planetary Science Letters*, 176, 7–16. [https://doi.org/10.1016/S0012-821X\(99\)00312-X](https://doi.org/10.1016/S0012-821X(99)00312-X)
- Abrantes, F., & Moita, M. T. (1999). Water column and recent sediment data on diatoms and coccolithophorids, off Portugal, confirm sediment record of upwelling events. *Oceanologica Acta*, 22, 319–336. [https://doi.org/10.1016/S0399-1784\(99\)80055-3](https://doi.org/10.1016/S0399-1784(99)80055-3)
- Alvarez, I., Gomez-Gesteira, M., DeCastro, M., Lorenzo, M., Crespo, A., & Dias, J. (2011). Comparative analysis of upwelling influence between the western and northern coast of the Iberian Peninsula. *Continental Shelf Research*, 31, 388–399. <https://doi.org/10.1016/j.csr.2010.07.009>

- Alvarez, I., Ospina-Alvarez, N., Pazos, Y., deCastro, M., Bernardez, P., Campos, M. J., et al. (2009). A winter upwelling event in the Northern Galician Rias: Frequency and oceanographic implications. *Estuarine, Coastal and Shelf Science*, 82, 573–582. <https://doi.org/10.1016/j.ecss.2009.02.023>
- Amore, F. O., Flores, J. A., Voelker, A. H. L., Lebreiro, S. M., Palumbo, E., & Sierro, F. J. (2012). A Middle Pleistocene Northeast Atlantic coccolithophore record: Paleoclimatology and paleoproductivity aspects. *Marine Micropaleontology*, 90–91, 44–59. <https://doi.org/10.1016/j.marmicro.2012.03.006>
- Andruleit, H., Stäger, S., Rogalla, U., & Čepeck, P. (2003). Living coccolithophores in the northern Arabian Sea: Ecological tolerances and environmental control. *Marine Micropaleontology*, 49(1–2), 157–181. [https://doi.org/10.1016/s0377-8398\(03\)00049-5](https://doi.org/10.1016/s0377-8398(03)00049-5)
- Ausin, B., Hernández-Almeida, I., Flores, J.-A., Sierro, F.-J., Grosjean, M., Francés, G., & Alonso, B. (2015). Development of coccolithophore-based transfer functions in the western Mediterranean sea: A sea surface salinity reconstruction for the last 15.5 kyr. *Climate of the Past*, 11, 1635–1651. <https://doi.org/10.5194/cp-11-1635-2015>
- Ausin, B., Hodell, D. A., Cutmore, A., & Eglinton, T. I. (2020). The impact of abrupt deglacial climate variability on productivity and upwelling on the southwestern Iberian margin. *Quaternary Science Reviews*, 230, 106139. <https://doi.org/10.1016/j.quascirev.2019.106139>
- Balestra, B., Grunert, P., Ausin, B., Hodell, D., Flores, J. A., Alvarez-Zarikian, C. A., et al. (2017). Coccolithophore and benthic foraminifera distribution patterns in the Gulf of Cadiz and western Iberian margin during Integrated Ocean Drilling Program (IODP) expedition 339. *Journal of Marine Systems*, 170, 50–67. <https://doi.org/10.1016/j.jmarsys.2017.01.005>
- Barker, S., Archer, D., Booth, L., Elderfield, H., Henderiks, J., & Rickaby, R. E. M. (2006). Globally increased pelagic carbonate production during the Mid-Brunhes dissolution interval and the CO₂ paradox of MIS 11. *Quaternary Science Reviews*, 25, 3278–3293. <https://doi.org/10.1016/j.quascirev.2006.07.018>
- Barton, E. D. (2001). Canary and Portugal Currents. In J. H. Steele (Ed.) *Encyclopedia of Ocean Sciences*, (pp. 380–389). Oxford: Academic Press. <https://doi.org/10.1006/rwos.2001.0360>
- Barton, E., Inall, M., Sherwin, T., & Torres, R. (2001). Vertical structure, turbulent mixing and fluxes during Lagrangian observations of an upwelling filament system off Northwest Iberia. *Progress in Oceanography*, 51, 249–267. [https://doi.org/10.1016/s0079-6611\(01\)00069-6](https://doi.org/10.1016/s0079-6611(01)00069-6)
- Baumann, K.-H., Böckel, B., Frenz, M. (2004). *Coccolith contribution to South Atlantic carbonate sedimentation, Coccolithophores*, pp. 367–402. Springer. https://doi.org/10.1007/978-3-662-06278-4_14
- Baumann, K.-H., & Freitag, T. (2004). Pleistocene fluctuations in the northern Benguela Current system as revealed by coccolith assemblages. *Marine Micropaleontology*, 52, 195–215. <https://doi.org/10.1016/j.marmicro.2004.04.011>
- Beaufort, L., Lancelot, Y., Camberlin, P., Cayre, O., Vincent, E., Bassinot, F., & Labeyrie, L. (1997). Insolation cycles as a major control of equatorial Indian Ocean primary production. *Science*, 278, 1451–1454. <https://doi.org/10.1126/science.278.5342.1451>
- Boeckel, B., & Baumann, K.-H. (2004). Distribution of coccoliths in surface sediments of the south-eastern South Atlantic Ocean: Ecology, preservation and carbonate contribution. *Marine Micropaleontology*, 51, 301–320. <https://doi.org/10.1016/j.marmicro.2004.01.001>
- Bradt Miller, L. I., McGee, D., Awalt, M., Evers, J., Yerxa, H., Kinsley, C. W., & deMenocal, P. B. (2016). Changes in biological productivity along the northwest African margin over the past 20,000 years. *Paleoceanography*, 31, 185–202. <https://doi.org/10.1002/2015pa002862>
- Cachão, M., Oliveira, A., & Vitorino, J. (2000). Subtropical winter guests, offshore Portugal. *Journal of Nanoplankton Research*, 22, 19–26.
- Candy, I., Schreve, D. C., Sherriff, J., & Tye, G. J. (2014). Marine Isotope Stage 11: Palaeoclimates, palaeoenvironments and its role as an analogue for the current interglacial. *Earth-Science Reviews*, 128, 18–51. <https://doi.org/10.1016/j.earscirev.2013.09.006>
- Cavaleiro, C., Voelker, A. H., Stoll, H., Baumann, K.-H., & Kucera, M. (2020). Coccolithophore productivity at the western Iberian Margin during the Middle Pleistocene (310–455 ka)–evidence from coccolith Sr/Ca data. *Climate of the Past*, 16, 2017–2037. <https://doi.org/10.5194/cp-16-2017-2020>
- Colmenero-Hidalgo, E., Flores, J.-A., Sierro, F. J., Bárcena, M. A., Löwemark, L., Schönfeld, J., & Grimalt, J. O. (2004). Ocean surface water response to short-term climate changes revealed by coccolithophores from the Gulf of Cadiz (NE Atlantic) and Alboran Sea (W Mediterranean). *Palaeogeography, Palaeoclimatology, Palaeoecology*, 205, 317–336. <https://doi.org/10.1016/j.palaeo.2003.12.014>
- Coste, B., Fiuza, A., & Minas, H. (1986). Conditions hydrologiques et chimiques associées à l’upwelling côtier du Portugal en fin d’été. *Oceanologica Acta*, 9, 149–158.
- de Abreu, L., Abrantes, F. F., Shackleton, N. J., Tzedakis, P. C., McManus, J. F., Oppo, D. W., & Hall, M. A. (2005). Ocean climate variability in the eastern North Atlantic during interglacial marine isotope stage 11: A partial analogue to the Holocene? *Paleoceanography*, 20(3). <https://doi.org/10.1029/2004pa001091>
- Desprat, S., Oliveira, D., Naughton, F., & Sánchez Goñi, M. F. (2017). L’étude du pollen des séquences sédimentaires marines pour la compréhension du climat: L’exemple des périodes chaudes passées. *Quaternaire. Revue de l’Association française pour l’étude du Quaternaire*, 28, 259–269. <https://doi.org/10.4000/quaternaire.8102>
- Elderfield, H., Ferretti, P., Greaves, M., Crowhurst, S., McCave, I. N., Hodell, D., & Piotrowski, A. M. (2012). Evolution of ocean temperature and ice volume through the mid-Pleistocene climate transition. *Science*, 337(6095), 704–709. <https://doi.org/10.1126/science.1221294>
- Expedition 339 Scientists. (2013). Site U1385. In D. A. V. Stow, F. J. Hernández-Molina, C. A. Alvarez Zarikian, & Expedition 339 Scientists (Eds.). *Proceedings of the integrated ocean drilling program*. 339. Tokyo: Integrated Ocean Drilling Program Management International, Inc. <https://doi.org/10.2204/iodp.proc.339.103.2013>
- Eynaud, F., De Abreu, L., Voelker, A., Schönfeld, J., Salgueiro, E., Turon, J. L., et al. (2009). Position of the Polar Front along the western Iberian margin during key cold episodes of the last 45 ka. *Geochemistry, Geophysics, Geosystems*, 10, Q07U05. <https://doi.org/10.1029/2009gc002398>
- Figueiras, F., Labarta, U., & Reiriz, M. F. (2002). Coastal upwelling, primary production and mussel growth in the Rias Baixas of Galicia. In *Sustainable increase of marine harvesting: fundamental mechanisms and new concepts*, pp. 121–131. Springer. https://doi.org/10.1007/978-94-017-3190-4_11
- Fiúza, A. F. (1983). *Upwelling patterns off Portugal, Coastal Upwelling its sediment record*. Springer, pp. 85–98. https://doi.org/10.1007/978-1-4615-6651-9_5
- Fiúza, A. F. G., Hamann, M., Ambar, I., Díaz del Río, G., González, N., & Cabanas, J. M. (1998). Water masses and their circulation off western Iberia during May 1993. *Deep Sea Research Part I: Oceanographic Research Papers*, 45, 1127–1160. [https://doi.org/10.1016/s0967-0637\(98\)00008-9](https://doi.org/10.1016/s0967-0637(98)00008-9)
- Flores, J. A., Bárcena, M. A., & Sierro, F. J. (2000). Ocean-surface and wind dynamics in the Atlantic Ocean off Northwest Africa during the last 140 000 years. *Palaeogeography, Palaeoclimatology, Palaeoecology*, 161, 459–478. [https://doi.org/10.1016/s0031-0182\(00\)00099-7](https://doi.org/10.1016/s0031-0182(00)00099-7)
- Flores, J. A., Gersonde, R., Sierro, F., & Niebler, H.-S. (2000). Southern Ocean Pleistocene calcareous nannofossil events: Calibration with isotope and geomagnetic stratigraphies. *Marine Micropaleontology*, 40, 377–402. [https://doi.org/10.1016/s0377-8398\(00\)00047-5](https://doi.org/10.1016/s0377-8398(00)00047-5)
- Flores, J. A., & Marino, M. (2002). Pleistocene calcareous nannofossil stratigraphy for ODP Leg 177 (Atlantic sector of the Southern Ocean). *Marine Micropaleontology*, 45, 191–224. [https://doi.org/10.1016/s0377-8398\(02\)00030-0](https://doi.org/10.1016/s0377-8398(02)00030-0)

- Flores, J. A., & Sierro, F. J. (1997). Revised technique for calculation of calcareous nannofossil accumulation rates. *Micropaleontology*, *43*, 321–324. <https://doi.org/10.2307/1485832>
- Flores, J. A., Sierro, F. J., Francés, G., Vázquez, A., & Zamarreno, I. (1997). The last 100,000 years in the western Mediterranean: Sea surface water and frontal dynamics as revealed by coccolithophores. *Marine Micropaleontology*, *29*, 351–366. [https://doi.org/10.1016/s0377-8398\(96\)00029-1](https://doi.org/10.1016/s0377-8398(96)00029-1)
- Gartner, S. (1988). Paleoceanography of the mid-Pleistocene. *Marine Micropaleontology*, *13*, 23–46. [https://doi.org/10.1016/0377-8398\(88\)90011-4](https://doi.org/10.1016/0377-8398(88)90011-4)
- Geisen, M., Billard, C., Broerse, A. T., Cros, L., Probert, I., & Young, J. R. (2002). Life-cycle associations involving pairs of holococcolithophorid species: Intraspecific variation or cryptic speciation?. *European Journal of Phycology*, *37*, 531–550. <https://doi.org/10.1017/s0967026202003852>
- Girardeau, J., Monteiro, P. M., & Nikodemus, K. (1993). Distribution and malformation of living coccolithophores in the northern Benguela upwelling system off Namibia. *Marine Micropaleontology*, *22*(1–2), 93–110.
- González-Lanchas, A., Flores, J.-A., Sierro, F. J., Bárcena, M. Á., Rigual-Hernández, A. S., Oliveira, D., et al. (2020). A new perspective of the Alboran Upwelling System reconstruction during the Marine Isotope Stage 11: A high-resolution coccolithophore record. *Quaternary Science Reviews*, *245*. art. no. 106520. <https://doi.org/10.1016/j.quascirev.2020.106520>
- Gouveia, C., Trigo, R. M., DaCamara, C. C., Libonati, R., & Pereira, J. M. (2008). The North Atlantic oscillation and European vegetation dynamics. *International Journal of Climatology: A Journal of the Royal Meteorological Society*, *28*, 1835–1847. <https://doi.org/10.1002/joc.1682>
- Grelaud, M., Schimmelmann, A., & Beaufort, L. (2009). Coccolithophore response to climate and surface hydrography in Santa Barbara Basin, California, AD 1917–2004. *Biogeosciences*, *6*(10), 2025–2039. <https://doi.org/10.5194/bg-6-2025-2009>
- Guerreiro, C., Sá, C., de Stigter, H., Oliveira, A., Cachão, M., Cros, L., et al. (2014). Influence of the Nazaré Canyon, central Portuguese margin, on late winter coccolithophore assemblages. *Deep Sea Research Part II: Topical Studies in Oceanography*, *104*, 335–358. <https://doi.org/10.1016/j.dsr2.2013.09.011>
- Haynes, R., & Barton, E. D. (1990). A poleward flow along the Atlantic coast of the Iberian Peninsula. *Journal of Geophysical Research*, *95*, 11425–11441. <https://doi.org/10.1029/jc095ic07p11425>
- Hernández, A., Cachão, M., Sousa, P., Trigo, R. M., Luterbacher, J., Vaquero, J. M., & Freitas, M. C. (2021). External forcing mechanisms controlling the North Atlantic coastal upwelling regime during the mid-Holocene. *Geology*, *49*(4), 433–437. <https://doi.org/10.1130/g48112.1>
- Hewitt, C. D., Broccoli, A. J., Mitchell, J. F., & Stouffer, R. J. (2001). A coupled model study of the last glacial maximum: Was part of the North Atlantic relatively warm? *Geophysical Research Letters*, *28*, 1571–1574. <https://doi.org/10.1029/2000gl012575>
- Hodell, D., Crowhurst, S., Skinner, L., Tzedakis, P. C., Margari, V., Channell, J. E., et al. (2013). Response of Iberian Margin sediments to orbital and suborbital forcing over the past 420 ka. *Paleoceanography*, *28*, 185–199. <https://doi.org/10.1002/palo.20017>
- Hodell, D., Lourens, L., Crowhurst, S., Konijnendijk, T., Tjallingii, R., Jiménez-Espejo, F., et al. (2015). A reference time scale for Site U1385 (Shackleton Site) on the SW Iberian Margin. *Global and Planetary Change*, *133*, 49–64. <https://doi.org/10.1016/j.gloplacha.2015.07.002>
- Hurrell, J. W. (1995). Decadal trends in the North Atlantic Oscillation: Regional temperatures and precipitation. *Science*, *269*, 676–679. <https://doi.org/10.1126/science.269.5224.676>
- Hurrell, J. W., Kushnir, Y., Ottersen, G., & Visbeck, M. (2003). An overview of the North Atlantic oscillation. *Geophysical Monograph-American Geophysical Union*, *134*, 1–35. <https://doi.org/10.1029/134gm01>
- Incarbona, A., Martrat, B., Di Stefano, E., Grimalt, J. O., Pelosi, N., Patti, B., & Tranchida, G. (2010). Primary productivity variability on the Atlantic Iberian Margin over the last 70,000 years: Evidence from coccolithophores and fossil organic compounds. *Paleoceanography*, *25*(2). <https://doi.org/10.1029/2008pa001709>
- Jansen, J. H. F., Kuijpers, A., & Troelstra, S. R. (1986). A Mid-Brunhes Climatic Event: Long-Term Changes in Global Atmosphere and Ocean Circulation. *Science*, *232*, 619–622. <https://doi.org/10.1126/science.232.4750.619>
- Jordan, R., & Winter, A. (2000). Assemblages of coccolithophorids and other living microplankton off the coast of Puerto Rico during January–May 1995. *Marine Micropaleontology*, *39*, 113–130. [https://doi.org/10.1016/s0377-8398\(00\)00017-7](https://doi.org/10.1016/s0377-8398(00)00017-7)
- Jouzel, J., Masson-Delmotte, V., Cattani, O., Dreyfus, G., Falourd, S., Hoffmann, G., et al. (2007). Orbital and millennial Antarctic climate variability over the past 800,000 years. *Science*, *317*, 793–796. <https://doi.org/10.1126/science.1141038>
- Keffer, T., Martinson, D., & Corliss, B. (1988). The position of the Gulf Stream during Quaternary glaciations. *Science*, *241*, 440–442. <https://doi.org/10.1126/science.241.4864.440>
- Kinkel, H., Baumann, K.-H., & Cepek, M. (2000). Coccolithophores in the equatorial Atlantic Ocean: Response to seasonal and Late Quaternary surface water variability. *Marine Micropaleontology*, *39*, 87–112. [https://doi.org/10.1016/s0377-8398\(00\)00016-5](https://doi.org/10.1016/s0377-8398(00)00016-5)
- Lang, N., & Wolff, E. W. (2011). Interglacial and glacial variability from the last 800 ka in marine, ice and terrestrial archives. *Climate of the Past*, *7*, 361–380. <https://doi.org/10.5194/cp-7-361-2011>
- Lebreiro, S., Moreno, J., McCave, I., & Weaver, P. (1996). Evidence for Heinrich layers off Portugal (Tore Seamount: 39 N, 12 W). *Marine Geology*, *131*, 47–56. [https://doi.org/10.1016/0025-3227\(95\)00142-5](https://doi.org/10.1016/0025-3227(95)00142-5)
- Lisiecki, L. E., & Raymo, M. E. (2005). A Pliocene-Pleistocene stack of 57 globally distributed benthic $\delta^{18}O$ records. *Paleoceanography*, *20*(1). <https://doi.org/10.1029/2004pa001071>
- Lopes, J. F., Cardoso, A. C., Moita, M. T., Rocha, A. C., & Ferreira, J. A. (2009). Modelling the temperature and the phytoplankton distributions at the Aveiro near coastal zone, Portugal. *Ecological Modelling*, *220*, 940–961. <https://doi.org/10.1016/j.ecolmodel.2008.11.024>
- Loutre, M.-F., & Berger, A. (2003). Marine Isotope Stage 11 as an analogue for the present interglacial. *Global and Planetary Change*, *36*, 209–217. [https://doi.org/10.1016/s0921-8181\(02\)00186-8](https://doi.org/10.1016/s0921-8181(02)00186-8)
- Maiorano, P., Marino, M., Balestra, B., Flores, J.-A., Hodell, D., & Rodrigues, T. (2015). Coccolithophore variability from the Shackleton Site (IODP Site U1385) through MIS 16–10. *Global and Planetary Change*, *133*, 35–48. <https://doi.org/10.1016/j.gloplacha.2015.07.009>
- Marino, M., Maiorano, P., Tarantino, F., Voelker, A., Capotondi, L., Giron, A., et al. (2014). Coccolithophores as proxy of seawater changes at orbital-to-millennial scale during middle Pleistocene Marine Isotope Stages 14–9 in North Atlantic core MD01-2446. *Paleoceanography*, *29*, 518–532. <https://doi.org/10.1002/2013pa002574>
- Marlowe, I. T., Brassell, S. C., Eglinton, G., & Green, J. C. (1990). Long-chain alkenones and alkyl alkenoates and the fossil coccolith record of marine sediments. *Chemical Geology*, *88*(3–4), 349–375. [https://doi.org/10.1016/0009-2541\(90\)90098-r](https://doi.org/10.1016/0009-2541(90)90098-r)
- Martin-Garcia, G. M., Alonso-Garcia, M., Sierro, F. J., Hodell, D. A., & Flores, J. A. (2015). Severe cooling episodes at the onset of deglaciations on the Southwestern Iberian margin from MIS 21 to 13 (IODP site U1385). *Global and Planetary Change*, *135*, 159–169. <https://doi.org/10.1016/j.gloplacha.2015.11.001>

- Martrat, B., Grimalt, J. O., Shackleton, N. J., de Abreu, L., Hutterli, M. A., & Stocker, T. F. (2007). Four climate cycles of recurring deep and surface water destabilizations on the Iberian margin. *Science*, *317*, 502–507. <https://doi.org/10.1126/science.1139994>
- Mason, E., Coombs, S., & Oliveira, P. (2005). An overview of the literature concerning the oceanography of the eastern North Atlantic region. *Relatórios Científicos e Técnicos IPIMAR Serie Digital*, *33*, 59.
- McCartney, M. S., & Talley, L. D. (1982). The subpolar mode water of the North Atlantic Ocean. *Journal of Physical Oceanography*, *12*, 1169–1188. [https://doi.org/10.1175/1520-0485\(1982\)012<1169:tsmwot>2.0.co;2](https://doi.org/10.1175/1520-0485(1982)012<1169:tsmwot>2.0.co;2)
- McManus, J. F., Oppo, D. W., & Cullen, J. L. (1999). A 0.5-million-year record of millennial-scale climate variability in the North Atlantic. *Science*, *283*, 971–975. <https://doi.org/10.1126/science.283.5404.971>
- Mix, A. C. (1989). Influence of productivity variations on long-term atmospheric CO₂. *Nature*, *337*, 541–544. <https://doi.org/10.1038/337541a0>
- Moita, M., Silva, A., Palma, S., & Vilarinho, M. (2010). The coccolithophore summer–autumn assemblage in the upwelling waters of Portugal: Patterns of mesoscale distribution (1985–2005). *Estuarine, Coastal and Shelf Science*, *87*, 411–419. <https://doi.org/10.1016/j.ecss.2010.01.025>
- Moita, T. (1993). Spatial variability of phytoplankton communities in the upwelling region off Portugal. *Proceeding of the International Council for the Exploration of the Sea L*, *64*, 1–20.
- Molfino, B., & McIntyre, A. (1990). Precessional forcing of nutricline dynamics in the equatorial Atlantic. *Science*, *249*, 766–769. <https://doi.org/10.1126/science.249.4970.766>
- Naafs, B. D. A., Hefter, J., Ferretti, P., Stein, R., & Haug, G. H. (2011). Sea surface temperatures did not control the first occurrence of Hudson Strait Heinrich Events during MIS 16. *Paleoceanography*, *26*(4). <https://doi.org/10.1029/2011pa002135>
- Naafs, B. D. A., Hefter, J., Grützner, J., & Stein, R. (2013). Warming of surface waters in the mid-latitude North Atlantic during Heinrich events. *Paleoceanography*, *28*, 153–163. <https://doi.org/10.1029/2012pa002354>
- Naughton, F., Goñi, M. S., Kageyama, M., Bard, E., Duprat, J., Cortijo, E., et al. (2009). Wet to dry climatic trend in north-western Iberia within Heinrich events. *Earth and Planetary Science Letters*, *284*, 329–342. <https://doi.org/10.1016/j.epsl.2009.05.001>
- Okada, H., & Honjo, S. (1973). The distribution of oceanic coccolithophorids in the Pacific. *Deep Sea Research and Oceanographic Abstracts*, *20*, 355–374. [https://doi.org/10.1016/0011-7471\(73\)90059-4](https://doi.org/10.1016/0011-7471(73)90059-4)
- Okada, H., & Wells, P. (1997). Late Quaternary nannofossil indicators of climate change in two deep-sea cores associated with the Leeuwin Current off Western Australia. *Palaeogeography, Palaeoclimatology, Palaeoecology*, *131*, 413–432. [https://doi.org/10.1016/s0031-0182\(97\)00014-x](https://doi.org/10.1016/s0031-0182(97)00014-x)
- Oliveira, D., Desprat, S., Rodrigues, T., Naughton, F., Hodell, D., Trigo, R., et al. (2016). The complexity of millennial-scale variability in southwestern Europe during MIS 11. *Quaternary Research*, *86*, 373–387. <https://doi.org/10.1016/j.yqres.2016.09.002>
- Oliveira, D., Desprat, S., Yin, Q., Naughton, F., Trigo, R., Rodrigues, T., et al. (2018). Unraveling the forcings controlling the vegetation and climate of the best orbital analogues for the present interglacial in SW Europe. *Climate Dynamics*, *51*, 667–686. <https://doi.org/10.1007/s00382-017-3948-7>
- Oliveira, P. B., Nolasco, R., Dubert, J., Moita, T., & Peliz, A. (2009). Surface temperature, chlorophyll and advection patterns during a summer upwelling event off central Portugal. *Continental Shelf Research*, *29*, 759–774. <https://doi.org/10.1016/j.csr.2008.08.004>
- Oppo, D., McManus, J., & Cullen, J. (1998). Abrupt climate events 500,000 to 340,000 years ago: Evidence from subpolar North Atlantic sediments. *Science*, *279*, 1335–1338. <https://doi.org/10.1126/science.279.5355.1335>
- Pailler, D., & Bard, E. (2002). High frequency palaeoceanographic changes during the past 140 000 yr recorded by the organic matter in sediments of the Iberian Margin. *Palaeogeography, Palaeoclimatology, Palaeoecology*, *181*, 431–452. [https://doi.org/10.1016/s0031-0182\(01\)00444-8](https://doi.org/10.1016/s0031-0182(01)00444-8)
- Palumbo, E., Flores, J. A., Perugia, C., Emanuele, D., Petrillo, Z., Rodrigues, T., et al. (2013a). Abrupt variability of the last 24 ka BP recorded by coccolithophore assemblages off the Iberian Margin (core MD03-2699). *Journal of Quaternary Science*, *28*, 320–328. <https://doi.org/10.1002/jqs.2623>
- Palumbo, E., Flores, J. A., Perugia, C., Petrillo, Z., Voelker, A., & Amore, F. (2013b). Millennial scale coccolithophore paleoproductivity and surface water changes between 445 and 360 ka (Marine Isotope Stages 12/11) in the Northeast Atlantic. *Palaeogeography, Palaeoclimatology, Palaeoecology*, *383*, 27–41. <https://doi.org/10.1016/j.palaeo.2013.04.024>
- Parente, A., Cachão, M., Baumann, K.-H., de Abreu, L., & Ferreira, J. (2004). Morphometry of *Coccolithus pelagicus* sl (Coccolithophore, Haptophyta) from offshore Portugal, during the last 200 kyr. *Micropaleontology*, *50*, 107–120. https://doi.org/10.2113/50.suppl_1.107
- Peliz, Á., Dubert, J., Santos, A. M. P., Oliveira, P. B., & Le Cann, B. (2005). Winter upper ocean circulation in the Western Iberian Basin—Fronts, Eddies and Poleward Flows: An overview. *Deep Sea Research Part I: Oceanographic Research Papers*, *52*, 621–646. <https://doi.org/10.1016/j.dsr.2004.11.005>
- Pérez, F. F., Castro, C. G., Álvarez-Salgado, X. A., & Ríos, A. F. (2001). Coupling between the Iberian basin — scale circulation and the Portugal boundary current system: A chemical study. *Deep Sea Research Part I: Oceanographic Research Papers*, *48*, 1519–1533. [https://doi.org/10.1016/s0967-0637\(00\)00101-1](https://doi.org/10.1016/s0967-0637(00)00101-1)
- Petit, J.-R., Jouzel, J., Raynaud, D., Barkov, N. I., Barnola, J.-M., Basile, I., et al. (1999). Climate and atmospheric history of the past 420,000 years from the Vostok ice core, Antarctica. *Nature*, *399*, 429–436. <https://doi.org/10.1038/20859>
- Railsback, L. B., Gibbard, P. L., Head, M. J., Voarintsoa, N. R. G., & Toucanne, S. (2015). An optimized scheme of lettered marine isotope substages for the last 1.0 million years, and the climatostratigraphic nature of isotope stages and substages. *Quaternary Science Reviews*, *111*, 94–106. <https://doi.org/10.1016/j.quascirev.2015.01.012>
- Relvas, P., Barton, E. D., Dubert, J., Oliveira, P. B., Peliz, A., Da Silva, J., & Santos, A. M. P. (2007). Physical oceanography of the western Iberia ecosystem: Latest views and challenges. *Progress in Oceanography*, *74*, 149–173. <https://doi.org/10.1016/j.pocean.2007.04.021>
- Ríos, A. F., Pérez, F. F., & Fraga, F. (1992). Water masses in the upper and middle North Atlantic Ocean east of the Azores. *Deep Sea Research Part A: Oceanographic Research Papers*, *39*(3–4), 645–658. [https://doi.org/10.1016/0198-0149\(92\)90093-9](https://doi.org/10.1016/0198-0149(92)90093-9)
- Rodrigues, T., Alonso-García, M., Hodell, D. A., Rufino, M., Naughton, F., Grimalt, J. O., et al. (2017). A 1-Ma record of sea surface temperature and extreme cooling events in the North Atlantic: A perspective from the Iberian Margin. *Quaternary Science Reviews*, *172*, 118–130. <https://doi.org/10.1016/j.quascirev.2017.07.004>
- Rodrigues, T., Grimalt, J. O., Abrantes, F. G., Flores, J. A., & Lebreiro, S. M. (2009). Holocene interdependences of changes in sea surface temperature, productivity, and fluvial inputs in the Iberian continental shelf (Tagus mud patch). *Geochemistry, Geophysics, Geosystems*, *10*, Q07U06. <https://doi.org/10.1029/2008gc002367>
- Rodrigues, T., Grimalt, J. O., Abrantes, F., Naughton, F., & Flores, J.-A. (2010). The last glacial–interglacial transition (LGIT) in the western mid-latitudes of the North Atlantic: Abrupt sea surface temperature change and sea level implications. *Quaternary Science Reviews*, *29*, 1853–1862. <https://doi.org/10.1016/j.quascirev.2010.04.004>

- Rodrigues, T., Voelker, A., Grimalt, J., Abrantes, F., & Naughton, F. (2011). Iberian Margin sea surface temperature during MIS 15 to 9 (580–300 ka): Glacial suborbital variability versus interglacial stability. *Paleoceanography*, 26(1). <https://doi.org/10.1029/2010pa001927>
- Rohling, E. J., Grant, K., Bolshaw, M., Roberts, A., Siddall, M., Hemleben, C., & Kucera, M. (2009). Antarctic temperature and global sea level closely coupled over the past five glacial cycles. *Nature Geoscience*, 2, 500–504. <https://doi.org/10.1038/ngeo557>
- Romero, O. E., Kim, J. H., & Donner, B. (2008). Submillennial-to-millennial variability of diatom production off Mauritania, NW Africa, during the last glacial cycle. *Paleoceanography*, 23(3). <https://doi.org/10.1029/2008pa001601>
- Ruddiman, W. F. (1977). Late Quaternary deposition of ice-rafted sand in the subpolar North Atlantic (lat 40 to 65 N). *Geological Society of America Bulletin*, 88, 1813–1827. [https://doi.org/10.1130/0016-7606\(1977\)88<1813:lqdois>2.0.co;2](https://doi.org/10.1130/0016-7606(1977)88<1813:lqdois>2.0.co;2)
- Ruddiman, W. F., & McIntyre, A. (1981). The mode and mechanism of the last deglaciation: Oceanic evidence. *Quaternary Research*, 16, 125–134. [https://doi.org/10.1016/0033-5894\(81\)90040-5](https://doi.org/10.1016/0033-5894(81)90040-5)
- Saavedra-Pellitero, M., Baumann, K. H., Lamy, F., & Köhler, P. (2017). Coccolithophore variability across Marine Isotope Stage 11 in the Pacific sector of the Southern Ocean and its potential impact on the carbon cycle. *Paleoceanography*, 32, 864–880. <https://doi.org/10.1002/2017pa003156>
- Salgueiro, E., Naughton, F., Voelker, A. H. L., de Abreu, L., Alberto, A., Rossignol, L., et al. (2014). Past circulation along the western Iberian margin: A time slice vision from the Last Glacial to the Holocene. *Quaternary Science Reviews*, 106, 316–329. <https://doi.org/10.1016/j.quascirev.2014.09.001>
- Sánchez Goñi, M. F. (2020). Regional impacts of climate change and its relevance to human evolution. *Evolutionary Human Sciences*, 2, e55. <https://doi.org/10.1017/ehs.2020.56>
- Sánchez Goñi, M. F., Llave, E., Oliveira, D., Naughton, F., Desprat, S., Ducassou, I., et al. (2016). Climate changes in south western Iberia and Mediterranean Outflow variations during two contrasting cycles of the last 1 Myrs: MIS 31-MIS 30 and MIS 12-MIS 11. *Global and Planetary Change*, 136, 18–29. <https://doi.org/10.1016/j.gloplacha.2015.11.006>
- Sarnthein, M., Winn, K., Duplessy, J.-C., & Fontugne, M. R. (1988). Global variations of surface ocean productivity in low and mid latitudes: Influence on CO₂. *Paleoceanography*, 3, 361–399. <https://doi.org/10.1029/pa003i003p00361>
- Schubert, C., Villanueva, J., Calvert, S., Cowie, G., Von Rad, U., Schulz, H., et al. (1998). Stable phytoplankton community structure in the Arabian Sea over the past 200,000 years. *Nature*, 394, 563–566. <https://doi.org/10.1038/29047>
- Schulte, S., Rostek, F., Bard, E., Rullkötter, J., & Marchal, O. (1999). Variations of oxygen-minimum and primary productivity recorded in sediments of the Arabian Sea. *Earth and Planetary Science Letters*, 173, 205–221. [https://doi.org/10.1016/s0012-821x\(99\)00232-0](https://doi.org/10.1016/s0012-821x(99)00232-0)
- Shackleton, N. J., Hall, M. A., & Vincent, E. (2000). Phase relationships between millennial-scale events 64,000–24,000 years ago. *Paleoceanography*, 15, 565–569. <https://doi.org/10.1029/2000pa000513>
- Silva, A., Palma, S., & Moita, M. (2008). Coccolithophores in the upwelling waters of Portugal: Four years of weekly distribution in Lisbon bay. *Continental Shelf Research*, 28, 2601–2613. <https://doi.org/10.1016/j.csr.2008.07.009>
- Silva, A., Palma, S., Oliveira, P., & Moita, M. (2009). Composition and interannual variability of phytoplankton in a coastal upwelling region (Lisbon Bay, Portugal). *Journal of Sea Research*, 62, 238–249. <https://doi.org/10.1016/j.seares.2009.05.001>
- Spratt, R. M., & Lisiecki, L. E. (2016). A Late Pleistocene sea level stack. *Climate of the Past*, 12(4), 1079–1092. <https://doi.org/10.5194/cp-12-1079-2016>
- Stein, R., Heftner, J., Grütznert, J., Voelker, A., & Naafs, B. D. A. (2009). Variability of surface water characteristics and Heinrich-like events in the Pleistocene midlatitude North Atlantic Ocean: Biomarker and XRD records from IODP Site U1313 (MIS 16–9). *Paleoceanography*, 24(2). <https://doi.org/10.1029/2008pa001639>
- Stolz, K., & Baumann, K. H. (2010). Changes in palaeoceanography and palaeoecology during Marine Isotope Stage (MIS) 5 in the eastern North Atlantic (ODP Site 980) deduced from calcareous nannoplankton observations. *Palaeogeography, Palaeoclimatology, Palaeoecology*, 292(1–2), 295–305. <https://doi.org/10.1016/j.palaeo.2010.04.002>
- Trigo, R. M., Osborn, T. J., & Corte-Real, J. M. (2002). The North Atlantic Oscillation influence on Europe: Climate impacts and associated physical mechanisms. *Climate Research*, 20, 9–17. <https://doi.org/10.3354/cr020009>
- van Aken, H. M. (2001). The hydrography of the mid-latitude northeast Atlantic Ocean—Part III: The subducted thermocline water mass. *Deep Sea Research Part I: Oceanographic Research Papers*, 48, 237–267. [https://doi.org/10.1016/s0967-0637\(00\)00059-5](https://doi.org/10.1016/s0967-0637(00)00059-5)
- Vautravers, M. J., & Shackleton, N. J. (2006). Centennial-scale surface hydrology off Portugal during marine isotope stage 3: Insights from planktonic foraminiferal fauna variability. *Paleoceanography*, 21(3). <https://doi.org/10.1029/2005pa001144>
- Villanueva, J., Calvo, E., Pelejero, C., Grimalt, J., Boelaert, A., & Labeyrie, L. (2001). A latitudinal productivity band in the central North Atlantic over the last 270 kyr: An alkenone perspective. *Paleoceanography*, 16, 617–626. <https://doi.org/10.1029/2000pa000543>
- Villanueva, J., Grimalt, J. O., Labeyrie, L. D., Cortijo, E., Vidal, L., & Louis-Turon, J. (1998). Precessional forcing of productivity in the North Atlantic Ocean. *Paleoceanography*, 13, 561–571. <https://doi.org/10.1029/98pa02318>
- Villanueva, J., Pelejero, C., & Grimalt, J. O. (1997). Clean-up procedures for the unbiased estimation of C37 alkenone sea surface temperatures and terrigenous n-alkane inputs in paleoceanography. *Journal of Chromatography*, 757, 145–151. [https://doi.org/10.1016/s0021-9673\(96\)00669-3](https://doi.org/10.1016/s0021-9673(96)00669-3)
- Vitorino, J., Oliveira, A., Jouanneau, J. M., & Drago, T. (2002). Winter dynamics on the northern Portuguese shelf. Part 1: Physical processes. *Progress in Oceanography*, 52, 129–153. [https://doi.org/10.1016/s0079-6611\(02\)00003-4](https://doi.org/10.1016/s0079-6611(02)00003-4)
- Voelker, A. H. L., De Abreu, L., Schönfeld, J., Erlenkeuser, H., & Abrantes, F. (2009). Hydrographic conditions along the western Iberian margin during marine isotope stage 2. *Geochemistry, Geophysics, Geosystems*, 10, Q12U08. <https://doi.org/10.1029/2009gc002605>
- Voelker, A. H. L., Rodrigues, T., Billups, K., Oppo, D. W., McManus, J. F., Stein, R., et al., 2010. Variations in mid-latitude North Atlantic surface water properties during the mid-Brunhes (MIS 9–14) and their implications for the thermohaline circulation. *Climate of the Past*, 6, 531–552.
- Volkman, J. K., Eglinton, G., Corner, E. D., & Forsberg, T. (1980). Long-chain alkenes and alkenones in the marine coccolithophorid *Emiliania huxleyi*. *Phytochemistry*, 19, 2619–2622. [https://doi.org/10.1016/s0031-9422\(00\)83930-8](https://doi.org/10.1016/s0031-9422(00)83930-8)
- Wanner, H., Brönnimann, S., Casty, C., Gyalistras, D., Luterbacher, J., Schmutz, C., et al. (2001). North Atlantic Oscillation—concepts and studies. *Surveys in Geophysics*, 22, 321–381. <https://doi.org/10.1023/a:1014217317898>
- Winter, A. (1994). Biogeography of living coccolithophores in ocean waters. *Coccolithophores*.
- Young, J. R., Bown, P. R., & Lees, J. A. (2020). *Nannotax3 website*. International Nannoplankton Association. Retrieved from <http://www.mikrotax.org/Nannotax3>. Accessed 10 Feb. 2021. URL.
- Young, J. R., Geisen, M., Cros, L., Kleijne, A., Sprengel, C., Probert, I., & Østergaard, J. (2003). A guide to extant coccolithophore taxonomy. *Journal of Nannoplankton Research, Special Issue, 1*, 1–132.